*GEOLOGICA CARPATHICA*, APRIL 2021, 72, 2, 114–133 https://doi.org/10.31577/GeolCarp.72.2.3

# Carboniferous mafic metavolcanic rocks in the Northern Gemeric Unit: Petrogenesis, geochemistry, isotope composition and tectonic implication

ANNA VOZÁROVÁ[1,✉], ONDREJ NEMEC[1], KATARÍNA ŠARINOVÁ[1], ROBERT ANCZKIEWICZ[2] and JOZEF VOZÁR[3]

[1]Comenius University in Bratislava, Faculty of Natural Sciences, Department of Mineralogy and Petrology, Mlynská dolina, Ilkovičova 6, 842 15 Bratislava, Slovakia; ✉anna.vozarova@uniba.sk, ondrej.nemec@uniba.sk, katarina.sarinova@uniba.sk
[2]Institute of Geological Sciences, Polish Academy of Sciences, Kraków Research Centre, Senacka 1, 31-002 Kraków, Poland; r.anczkiewicz@ingpan.krakow.pl
[3]Earth Science Institute of the Slovak Academy of Sciences, Dúbravská cesta 9, P.O. Box 106, 840 05 Bratislava, Slovakia; jozef.vozar@savba,sk

*(Manuscript received November 25, 2020; accepted in revised form March 25, 2021; Associate Editor: Igor Broska)*

**Abstract:** The paper presents whole rock chemical composition and Sr–Nd isotope data from selected metabasic rocks from the Mississippian and Pennsylvanian sequences of the Northern Gemeric Unit. The analysed metabasic rocks belong to the subalkaline magmatic series with Nb/Y ratios ranging from 0.03 to 0.21. They fit into the low-Ti tholeiitic series, characterized by $TiO_2$ contents of less than 2.5 wt. % and Ti/Y ratios below 500. Petrological and chemical signatures show the separation of the Group I (Pennsylvanian) from the Group II (Mississippian) metabasalts, which is supported by biostratigraphical data of the surrounding metasediments. The Group I metabasalts display higher contents of Zr, Th, Rb and U, Pb, Zn, Ni compared to the metabasalts of Group II and conversely lower contents of Nb, Ta and V. The chondrite normalized rare earth elements curves show a uniform pattern, with rare earth element enrichment and no or weak positive or negative Eu anomalies (0.88–1.23 vs. 0.89–1.17). The $(Tb/Yb)_N$ ratios from 1.36–1.62 in the Group I or 0.92–1.55 in Group II are symptomatic of spinel-bearing peridotite mantle source. Based on trace and rare earth element distribution patterns, the Group I metabasites correspond to the N-MORB/E-MORB field and the Group II metabasites shift significantly towards the BABB and CAB fields. The Sr/Nd isotope systematics confirmed depleted mantle isotopic signatures, with minor influences from crustal sources and affected by fluid-related subduction metasomatism. All the studied samples have positive $\varepsilon Nd_{(0)}$ ranging from 7.92 to 8.68 for Group I and from 4.59 to 10.52 for Group II metabasalts. The $^{87}Sr/^{86}Sr_{(0)}$ values vary between 0.7053–0.7081 and between 0.7052–0.7076, respectively, and 0.7109 for basaltic andesite.

**Keywords:** Mississippian and Pennsylvanian metabasalts, petrology, geochemistry, Sr–Nd isotope composition.

## Introduction

Generally, the Northern Gemeric Unit (NGU) Carboniferous sequences were strongly tectonically reduced during the multiphase development in the Alpine orogeny. For this reason, their complete stratigraphic records have not been preserved in today's tectonic fabric and therefore the position of the basic metavolcanics and their original relations to the immediate stratigraphic underlier and overlier are often insufficiently documented or at least discussed. Fragments of the basic metavolcanic rocks were found in both, the Mississippian and Pennsylvanian Series (Fig. 1).

The first complete lithostratigraphic classification of the NGU Carboniferous rock complexes was made by Bajaník et al. (1981), and it was also used in compiling the geological map of the Slovenské rudohorie Mts. – the eastern part at a scale of 1:50,000 and its explanation (Bajaník et al. 1983, 1984). The authors defined the Dobšiná Group and within it four formations: the Ochtiná, Rudňany, Zlatník and Hámor formations, in order from the stratigraphic bottom to the top. Later investigation has shown the need to redefine this lithostratigraphic scheme. The oldest Ochtiná Formation was separated from the Dobšiná Group and redefined as a separate lithostratigraphic unit of a higher order – the Ochtiná Group (Vozárová 1996). The main reason for such a definition splitting was their different geodynamic development and position within the Variscan orogeny and especially the significant break in sedimentation between the sequences of the Mississippian Ochtiná Group and the Pennsylvanian formations of the Dobšiná Group.

The last redefinition of Carboniferous sequences, on the other hand, concerned the Dobšiná Group. Ivan (1997) and Ivan & Méres (2012) distinguished and redefined the Zlatník Formation (ZF) rock complex. The authors removed the sequence of metabasic rocks from the upper part of the originally defined ZF as a new lithostratigraphic unit, the Zlatník Group. It should be noted that in the thrust fault and thrust sheet zone in the NGU Alpine structure, all contacts of rigid complexes such as volcanic rocks and relatively soft metasediments are tectonized. In fact, the occurrences of the ZF are located in

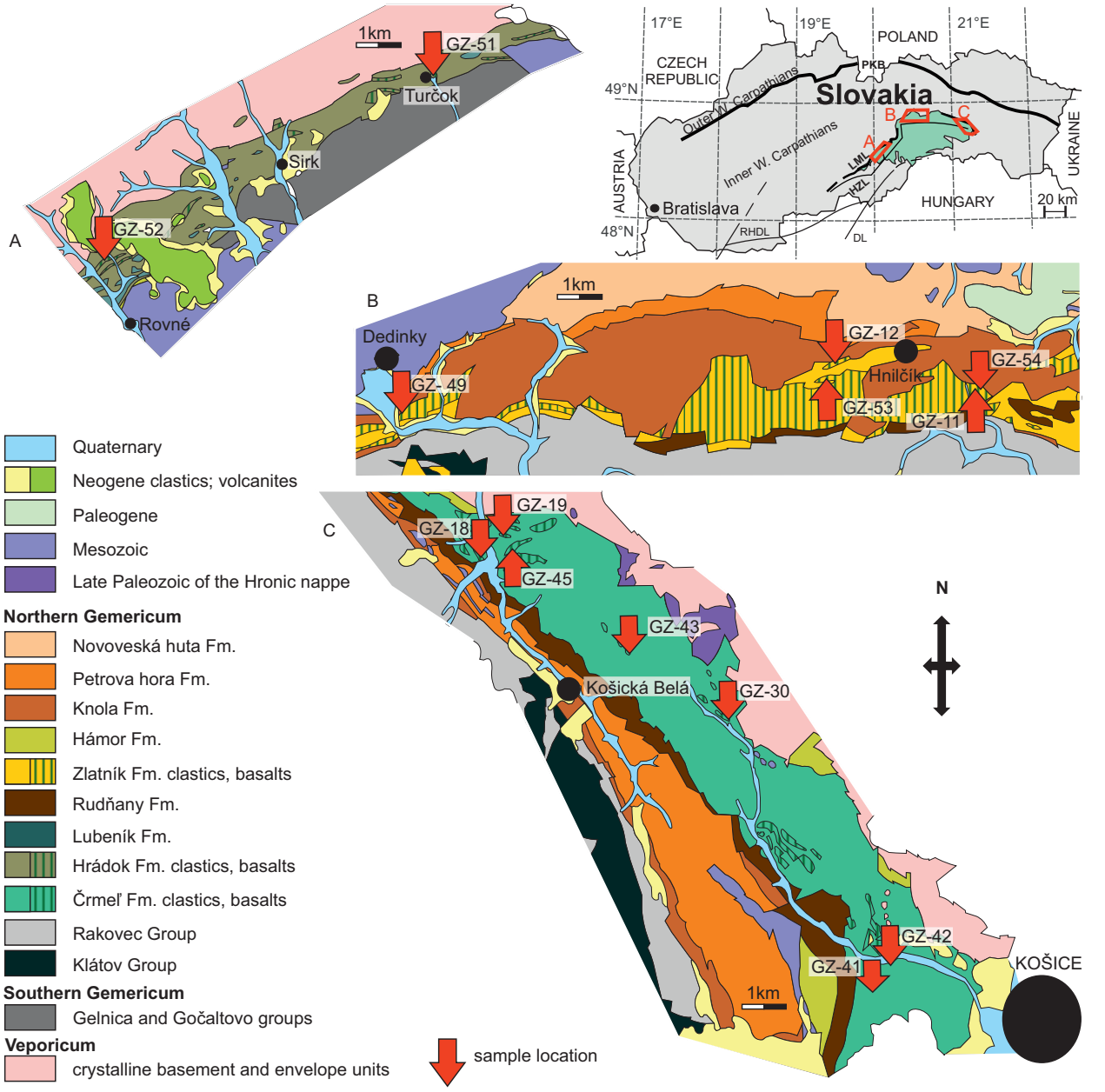


**Fig. 1.** Excerpts of details from the Geological map of the Slovenské rudohorie Mts. – eastern part, 1:50,000 (modified after Bajaník et al. 1984 and Polák & Jacko 1996 and adapted from the authors' manuscript materials), showing localities of the studied samples.

an imbricated structure between Dobšiná and Poráč (Mlynky thrust fault zone after Reichwalder & Snopko in Bajaník et al. 1983). Here, the tectonic scales of the ZF basic members and metasediments together with the Permian sediments are tectonically repeated several times above each other (see geological map Bajaník et al. 1984). Finally, it is not correct at all to accept the same geographical name of an earlier defined lithostratigraphic unit for a newly defined one. At this point it should be mentioned that ZF metabasic rocks were originally considered to be a part of the pre-Carboniferous basement, most likely of the low-grade Rakovec Group (termed as the Phyllite–Diabase Serie at that time, e.g. Kamenický & Marková 1957; Máška 1959; Fusán 1957 and others). However, some authors have incorporated this complex of metabasic rocks into the Carboniferous, e.g. Ogurčák (1954) and Hudáček (1963) in the area of Mlynky; Pecho & Popreňák (1962) from the area of Rudňany–Závadka; Rozložník (1963) from the area of Dobšiná. The authors of the geological map of the Slovenské rudohorie Mountains – eastern part (Bajaník et al. 1984) also agreed with this concept. The main geological reason why they were included in the Carboniferous was the lower degree of structural reworking compared to the rocks of the Rakovec Group, the close spatial connection with the Carboniferous sequence and the detection of the Carboniferous microflora in the associated metasediments (Snopková 1978a).

The presented article aims to bring new petrological, chemical and isotope data from the NGU Carboniferous metabasic rocks and their mutual comparison. Consequently, the data contribute to their genetic development, leading to a new geological and tectonic interpretations.

## Geological background and characteristics of Carboniferous formations

The Northern Gemericum Unit belongs to the pre-Gosau northward stacking crustal scale nappe system of the Western Carpathians (Biely et al. 1996; Plašienka 2018 and references therein). The NGU fits into the innermost part of the Alpine Central Western Carpathians, and as a whole it clearly overthrust the Veporicum Unit in its footwall, along the Alpine thrust nappe contact recognized as the Lubeník–Margecany Line (defined by Andrusov 1959). Similarly, further to the south, tectonic contact of the NGU with the adjacent Southern Gemericum Unit is represented by the Hrádok–Železník Line (defined by Abonyi 1971). The extreme Early Cretaceous shortening due to the nappe stacking is characteristic of the innermost part of the Central Western Carpathians. Due to this fact, the complexes preserved in the NGU synclinorial structure (Maheľ 1983) are generally characterized by the strong tectonic reduction and shortening.

The NGU zone encloses some relics of the Variscan subduction–collision suture, represented by the thrust wedges of the two pre-Carboniferous complexes (the higher-grade Klátov and low-grade Rakovec terranes), and fragments of Mississippian deep-water turbidite sequences. Post-Variscan deposition includes fan delta/shallow-marine to proximal delta Pennsylvanian (Bashkirian–Lower Moscovian) and continental Permian sequences (Rozložník 1963; Bajaník et al. 1981, 1983; Vozárová & Vozár 1988, Németh et al. 2004; Radvanec et al. 2017 and references therein). With respect to the Variscan tectonothermal events the NGU basement is subdivided into the gneiss–amphibolite complex of the *Klátov Terrane (KT)*, which includes some relics of the retrogressed eclogites, and the low-grade *Rakovec Terrane (RT),* predominantly composed of the tholeiitic metabasalts and metavolcaniclastics associated with a smaller amount of sandy–pelitic and Fe-rich metasediments and small bodies of metagabbro–diorites and keratophyres with geochemical characteristics near to E-MORB/OIT, BABB and island arc basalts (Bajaník 1976; Bajaník et al. 1983; Spišiak et al. 1985; Hovorka et al. 1988, 1997; Ivan 1994, 2009; Németh 2002; Németh et al. 2004; Radvanec et al. 2017; Faryad et al. 2020 and references therein).

Deformational and metamorphic events recorded in both pre-Carboniferous terranes occurred in the Late Devonian–Mississippian which is documented by their reworked rock fragments within the overstepping Pennsylvanian conglomerates (Krist 1954; Vozárová 1973, 2001) and by several geochronological data (Vozárová et al. 2005, 2013, 2019a; Putiš et al. 2009a). These rock complexes experienced Alpine reworking (Dallmeyer et al. 1996, 2005; Vozárová et al. 2005, 2014; Putiš et al. 2009b).

### *Mississippian*

Syn-orogenic Mississippian basins reflect the Variscan subduction–collision orogeny. In general, Devonian–Lower Carboniferous metamorphic and magmatic processes gave rise to an unequal consolidated continental crust that was further deformed during the post-collisional relaxation.

The syn-orogenic Tournaisian–Visean Ochtiná Group have been preserved as tectonic relics at the SW and E-SE boundary of the NGU. Despite the orogenic/metamorphic reduction the present thickness is estimated to be >1000 m (Vozárová 1996). The Mississippian turbidite wedges, presumably derived from the Variscan suture, were interpreted as the fill of an intrasuture remnant ocean basin (Vozárová & Vozár 1988) or foredeep basin (Neubauer & Vozárová 1990; Ebner et al. 2008).

The Hrádok Formation (Fm.) consists of a dark-grey and black clastic turbidite sequence, consisting of metaparaconglomerates, metasandstones, and metapelites, interlayered with basic metavolcaniclastics and also accompanied by olistoliths of metabasalts, metamicrodolerites and scarce amphibolites. Sporadic lydites and siliceous metapelites were found only in thin layers and lenses. Slabs of ultramafic rocks represented by the antigorite serpentinites and tremolite-talc schists are integral parts of this deep-water turbidite slope/rise olistostrome sequence. A monotonous complex of dark-grey and black metapelites, overlying the relatively coarser-grained lower part of the Hrádok Fm., yielded a microflora indicating the Upper Turnaisian–Visean age (Bajaník & Planderová 1985).

The Mississippian sequence of the Črmeľ Fm. represents a distal turbidite complex consisting of alternating metapelites, fine-grained metasandstones, basic to intermediate metavolcanics and its metavolcaniclastics, subsidiary allodapic carbonates and lydites (Bajaník et al. 1984; Grecula 1998). A small amount of acid volcaniclastic detritus is unevenly dispersed in its basal part. The Tournaisian–Visean age of the Črmeľ Fm. is indicated based on microflora assemblages (Snopková 1978b).

The overall upward-shallowing Mississippian sequence is interpreted to reflect the progressive basin filling. The youngest Mississippian sedimentary rocks (Lubeník Fm.; Vozárová 1996) are represented by the Upper Visean–Serpukhovian black shales and bioclastic carbonates, mostly metasomatically transformed to magnesites and dolomites. This horizon is well documented by fauna, mainly in the western part of their occurrences (trilobites – Bouček & Přibyl 1960; conodonts – Kozur et al. 1976; bryozoan – Zágoršek & Macko 1994; algae – Mamet & Mišík 2003).

### *Pennsylvanian*

The Pennsylvanian transgressive sequence of the Dobšiná Group rests unconformably on both the NGU pre-Carboni-

ferous complexes (Klátov and Rakovec) and on the Mississippian succession of the Črmeľ Fm. in the E-SE realm of the NGU (Fig. 1). This fix up the Variscan thrust/nappe structure. The Upper Bashkirian–Moscovian sequence started after a break of sedimentation with a boulder to coarse-grained delta-fan conglomerates (the Rudňany Fm.). They contain detritus derived from both pre-Carboniferous complexes (Klátov and Rakovec), as well as, from the Mississippian Črmeľ Fm. metasedimentary rocks (Krist 1954; Vozárová 1973; Vozárová & Vozár 1988). However, sporadic "exotic rocks" were found which do not occur on the NGU surface today. They include pebbles of plagiogranites, granitoides, orthogneisses and metaquartzites (Vozárová 1973, 2001, 2005; Vozárová et al. 2019a). Black shales and mica-rich grey sandstone intercalations are a normal member of the fining upward Rudňany Fm. They contain Pennsylvanian macroflora remains determined by Němejc (1947). The 370–380 Ma $^{40}Ar/^{39}Ar$ cooling age data of white mica from metasandstones and gneiss pebbles indicate the first step of Variscan collisional suturing in the NGU zone (Vozárová et al. 2005). After initial rapid sedimentation, the littoral to shallow-neritic limestones were associated with grey and black shales. This siliciclastic–carbonate lithofacies corresponds to the basal part of the Zlatník Fm. Its Moscovian age is indicated by rich trilobite (Rakusz 1932; Bouček & Přibyl 1960) and conodont fauna (Kozur & Mock 1977). The upper part of the Zlatník Fm. comprises fine-grained clastic metasediments associated with prevailing aphanitic metabasalts and their metavolcaniclastics. Poor microfloral assemblages proved the Pennsylvanian age from the associated black shales, but not an accurate division (Snopková 1978a). Termination of the Pennsylvanian peripheral basin is reflected by the paralic sequence of the Hámor Fm. It is characterized by distinct cyclical coarsening-upward shaly–sandy–conglomeratic sediments, an absence of synsedimentary volcanism and a local occurrence of ribbed coal seam. Poor microflora assemblages proved the uppermost Moscovian age (Planderová & Vozárová 1982).

## Analytical methods

A total of 15 samples were collected; their location is shown in Fig. 1 and Table 1.

The rock samples have been analysed for whole-rock chemical composition in the Bureau Veritas Commodities Canada Ltd. (former ACME Analytical Laboratories Ltd., Canada). Following a lithium metaborate/tetraborate fusion and dilute nitric digestion, major elements were determined by inductively coupled plasma (ICP-ES) and trace and rare elements (REE) by inductively coupled plasma mass spectrometry (ICP-MS). The analytical accuracy was controlled using geological standard materials and is estimated to be within a 0.01 % error (1σ, relative) for major elements, and within a 0.1–0.5 ppm error range (1σ, relative) for trace elements and 0.01–0.05 ppm for REEs.

Samples for Sr and Nd isotope analyses were chemically prepared and measured in the Isotope Geochemistry Laboratory at the Institute of Geological Sciences Polish Academy of Science, Krakow, according to procedures outlined in Anczkiewicz & Anczkiewicz (2016). Isotopic ratios of Nd were normalized to $^{143}Nd/^{144}Nd=0.7219$ to correct for mass bias. Reproducibility of Nd standard JNd- was $^{143}Nd/^{144}Nd=0.512101\pm8$ (2 s.d. n=3). Isotopic composition of Sr was normalized to $^{86}Sr/^{88}Sr=0.1194$ to correct for mass bias. Reproducibility of Sr standard SRM 987 during the analytical session was $^{87}Sr/^{86}Sr=0.710261\pm8$ (2 s.d. n=3). Mass bias corrections were conducted using the exponential law of Russel et al. (1978). The εNd values were calculated with parameters for CHUR $^{143}Nd/^{144}Nd=0.512638$, $^{147}Sm/^{144}Nd=0.1967$ (Jacobsen & Wasserburg 1980; DePaolo 1981).

Mineral analyses were carried out on a CAMECA SX-100 microprobe in the Laboratory of electro-optical methods of the State Dionýz Štúr Geological Institute in Bratislava.

Amphibole crystallochemical formulae were calculated using Excel spreadsheets by Locock et al. (2014) based on the nomenclature of Hawthorne et al. (2012). Recalculation of crystal formulae and classification of chlorites was carried out by Windows program WinCcac (Yavuz et al. 2015).

For Chl–Ph–Qtz–$H_2O$ multiequilibria geothermobarometry the MathWorks MATLAB script of Vidal et al. (2006) was used with Std state and solid solutions of Vidal et al. (2006) and Parra et al. (2002) for chlorite and Dubacq et al. (2010) for mica. Calculations were performed under the NCKFMASHO ($Na_2O$–CaO–$K_2O$–FeO–MgO–$Al_2O_3$–$SiO_2$–$H_2O$) chemical system using α-quartz, mica end-members: muscovite, Mg and Fe-celadonite and chlorite end-members: clinochlore, daphnite, sudoite, Mg and Fe-amesite, pyrophyllite. Water activity of $H_2O=1$ was used for calculations of all samples.

In addition, multi-equilibria geothermobarometry was followed by using chlorite thermometry of Cathelineau (1988) and Jowett (1991) based on $Al^{VI}$ with the Fe/(Fe+Mg) correction factors.

## Results

### *Petrology and mineralogy*

*Hrádok Formation metabasalts*: Mafic rocks were found in the Hrádok Formation (HF) in two forms. In its lower part they appear in the form of olistoliths in the turbidite sequence and then in situ, in its upper part, where they form basalt and dolerite bodies associated with dark metapelites. Volcanic rocks from the top of this pile were preferably selected for the analysis. In general, the studied rocks are pressure deformed. The original phenocrystals are flattened and replaced along the edges by a newly formed mineral association. The main part of the texture is formed by a fine-grained aggregate of newly formed metamorphic minerals with variable altered relics of magmatic hornblendes and plagioclases (Fig. 2A).

**Table 1:** List of studied rock samples and their locations.

| Sample No. | Lithostratigraphic unit | Age | Location | GPS coordinates |
|---|---|---|---|---|
| *GZ-49* | Zlatník Formation | Pennsylvanian | roadcut at the dam Dedinky | 48°51.243' N 20°23.149' E |
| *GZ-53* | Zlatník Formation | Pennsylvanian | Grajnár quarry, left side, 774 m a.s.l. | 48°52.357' N 20°31.508' E |
| *GZ-54* | Zlatník Formation | Pennsylvanian | roadcut Bindt-Hnilčík, 744 m a.s.l. | 48°51.963' N 20°34.092' E |
| *GZ-11* | Zlatník Formation | Pennsylvanian | roadcut Bindt-Hnilčík, 664 m a.s.l. | 48°51.955' N 20°34.013' E |
| *GZ-12* | Zlatník Formation | Pennsylvanian | Grajnár quarry, 850 m a.s.l. | 48°52.352' N 20°31.486' E |
| *GZ-51 A, B* | Hrádok Formation | Mississippian | NE from Turčok, Uhliarska Valley, 328 m a.s.l. | 48°38.488' N 20°08.911' E |
| *GZ-52* | Hrádok Formation | Mississippian | SW from Sušanský vrch elev. point, 470 m a.s.l. | 48°35.693' N 20°02.559' E |
| *GZ-18* | Črmeľ Formation | Mississippian | W of the Ružín dam, forest road, 400 m a.s.l. | 48°83.602' N 21°07.120' E |
| *GZ-19* | Črmeľ Formation | Mississippian | Ružín dam, roadcut Košické Hámre-Malá Lodina, 450 m a.s.l. | 48°83.771' N 21°07.570' E |
| *GZ-30* | Črmeľ Formation | Mississippian | Črmeľ valley, NW from Košice, 343 m a.s.l. | 48°45.106' N 21°12.697' E |
| *GZ-41 A, B* | Črmeľ Formation | Mississippian | Jahodná range, SE from 513 elev. point, 430 m a.s.l. | 48°44.635' N 21°12.398' E |
| *GZ-42* | Črmeľ Formation | Mississippian | roadcut Košise-Bankov, 600 m S from 426 elev. point, 357 m a.s.l. | 48°45.048' N 21°12.601' E |
| *GZ-43* | Črmeľ Formation | Mississippian | SE from Košická Belá Village, 495 m a.s.l. | 48°48.740' N 21°07.536' E |
| *GZ-45* | Črmeľ Formation | Mississippian | forest road Košické Hámre-Malá Lodina, 362 m a.s.l. | 48°49.997' N 21°04.559' E |

Remains of micro dolerite texture are preserved in the relics (Fig. 2B).

Two generations of amphiboles were distinguished, (i) relics of magmatic amphibole phenocrysts, and (ii) fine crystals of preferably oriented metamorphic amphiboles. Among the magmatic amphibole relics, the Mg-hornblendes (after Hawthorne et al. 2012) are dominant (Fig. 3A,B; Supplementary Table S1), with *mg#* varying from 0.57 to 0.69. Of the analysed hornblendes, only one from them corresponds to ferro-hornblende. The simple substitution Mg↔Fe is of prime importance within the studied hornblendes. Some magmatic hornblendes chemically correspond to pargasite as is indicated by the addition of Na on the *A* site and the substitution of Al for Si (Fig. 3; Supplementary Table S1). In addition to phenocrystals of hornblende, relics of the original crystals of igneous plagioclase are rarely preserved. They are strongly altered, especially replaced by albite. Residues of the anorthite component are retained within them, but not more than 15 % An (Supplementary Table S2).

The assemblage of metamorphic minerals is characterized by lepidonematoblastic texture with preferred orientation of actinolite/tremolite+chlorite+albite+epidote/zoizite crystalline aggregate, associated with small amounts of quartz and titanite. Compared to the magmatic hornblende, metamorphic amphibole is richer in $SiO_2$ (51–55 wt. %) and significantly poorer in $Al_2O_3$ (1.3–4.28 wt. %). According to the Hawthorne et al. (2012) classification, all the metamorphic amphiboles belong to the actinolite/tremolite group, with *mg#* ranging between 0.66 and 0.78. Low content of Na+K in *A* site (0.0–0.5 *a.p.f.u.*) is characteristic. The chemical composition of the associated chlorite corresponds to Clinochlore (after Zane & Weiss 1998), with *mg#* in the range from 0.53 to 0.65 (Fig. 4; Supplementary Table S3). The content of other cations is negligible or zero, with the exception of Mn, taking content from 0.39 to 0.26 *a.p.f.u.*

The composition of the associated metamorphic feldspars corresponds to pure albite (Supplementary Table S2). An epidote is an important component in the whole crystalline aggregate. Epidote forms euhedral crystals, mantled by chlorite and tremolite and it occurs in direct contact with albite and quartz.

*Črmeľ Formation metabasalts*: Metabasalts of the Črmeľ Formation correspondingly contain relics of the original magmatic phenocrysts in the inside of a newly formed aggregate of metamorphic minerals. Dominant lepidonematoblastic texture contains relics of magmatic amphibole and isolated plagioclase crystals (Fig. 2A). Relics of magmatic plagioclase are strongly saussuritized and albitized. The remnants of the An component remained, up to a maximum of 14 %, only in isolated smears (Supplementary Table S2).

Compared to samples from the Hrádok Formation metabasalts, the amphibole phenocrystals are preserved in the Črmeľ Formation metabasalts less frequently. Based on their chemical composition, they belong to the hornblende group and form a continuous series between Mg-hornblende and Mg-hastingsite (after Hawthorne et al. 2012; Fig. 3B; Supplementary Table S1), with the *mg#* varying from 0.53 to 0.59. The main difference between them is the relatively higher addition of Na in the *A* site (0.48–0.55 *a.p.f.u.*) and likewise

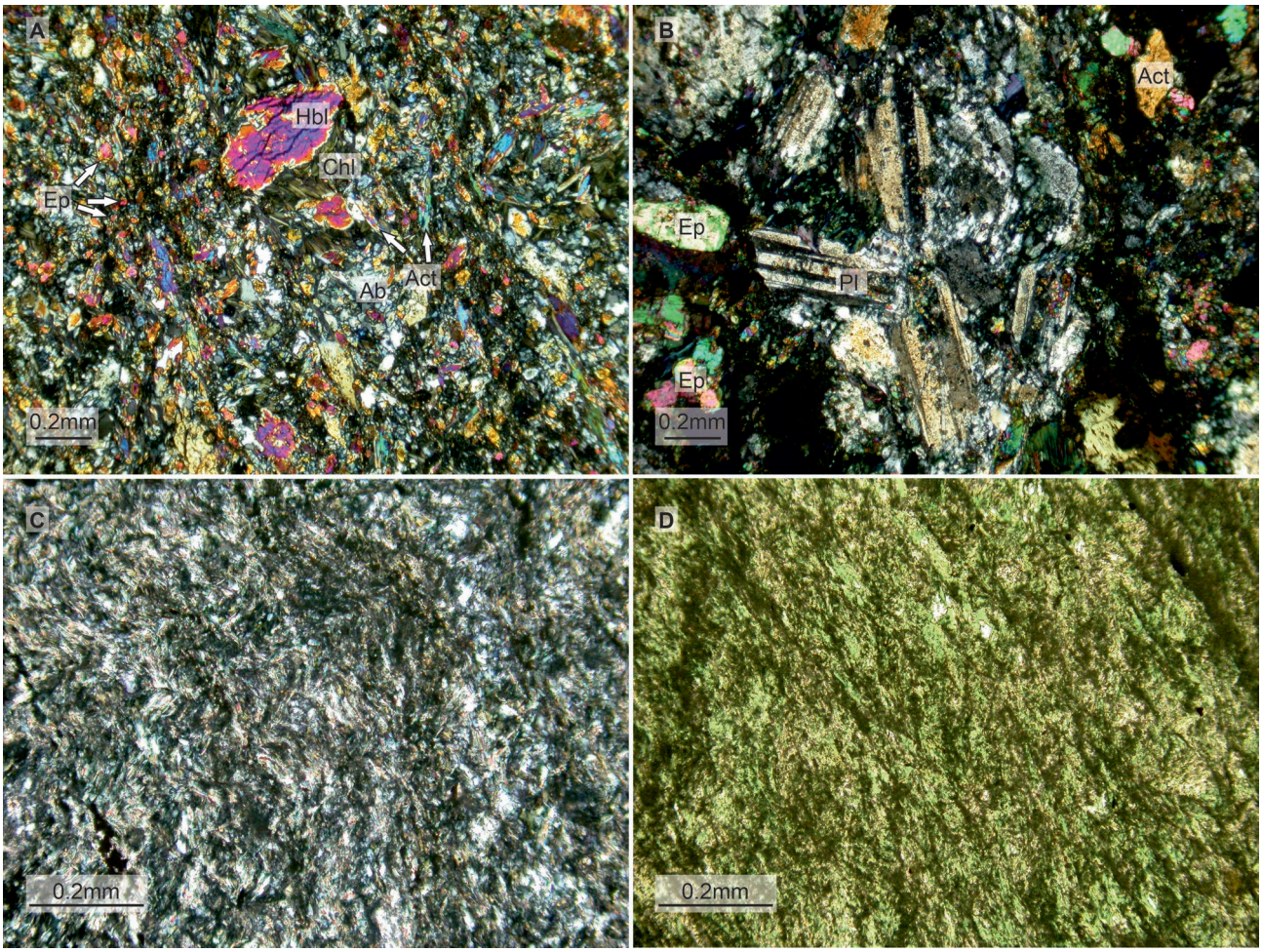


**Fig. 2.** Photomicrographs of the NGU Carboniferous metabasites: **A** — Mississippian metabasalt texture (sample GZ-52) with relics of magmatic amphiboles (Hbl) and aggregate of metamorphic minerals Act/Tr+Chl+Ep+Ab (cross-polarized light); **B** — Mississippian metabasalt texture (sample GZ-43) with relic of microdoleritic texture (cross-polarized light); **C** — Pennsylvanian metabasalts texture (sample GZ-54) made up of microlepidogranoblastic texture with aggregate of metamorphic minerals Chl+Ab+Ep±Mus, Cal and Fe–Ti oxides (cross-polarized light); **D** — Pennsylvanian metabasalt (sample GZ-11) with relics of small altered plagioclase laths (polarized light).

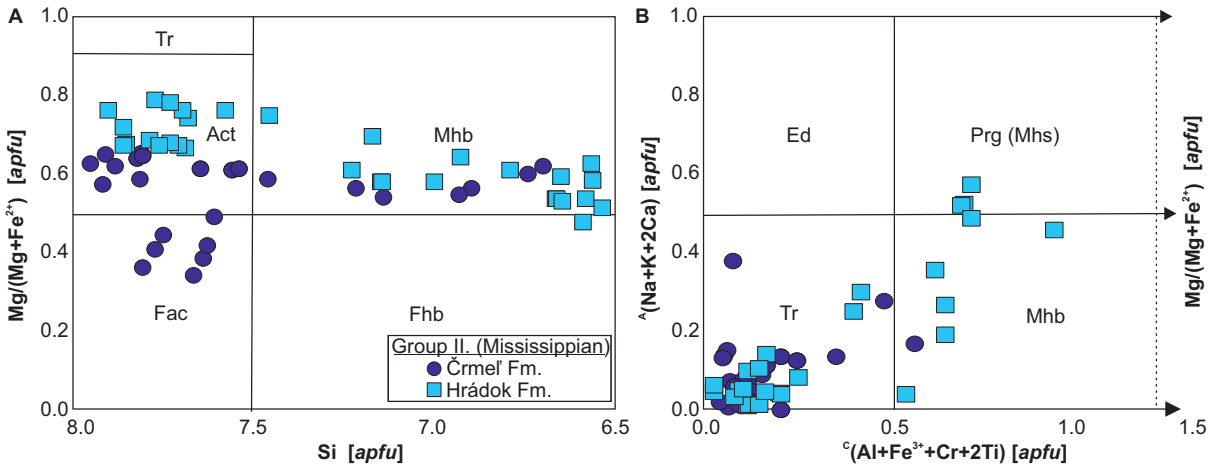


**Fig. 3.** Classification diagram of amphiboles: **A** — according to Leake et al. (1997); **B** — Hawthorne et al. (2012).

the higher $TiO_2$ content (1.8–2.2 wt. %) in the Mg-hastingsite (Supplementary Table S1). Magmatic hornblendes are replaced by actinolite/tremolite along the edges. This group of amphiboles is a part of the metamorphic mineral association in the matrix, which consists of actinolite/tremolite+epidote+albite+chlorite and less common titanite, white mica, quartz and carbonates. The studied actinolite/tremolite amphiboles are characterized by the $Fe^{2+}\leftrightarrow Mg^{2+}$ substitution, with *mg#* ranging between 0.48 and 0.65 (Fig. 3A,B; Supplementary Table S1). Their characteristics include low contents of $Al_2O_3$, varying from 0.91 to 4.06 wt. %, likewise very low content of Na in *A* site (maximally 0.10 *a.p.f.u.*). The content of other cations is negligible or zero. Associated chlorite corresponds to Chamosite (after Zane & Weiss 1998), with *mg#* in the range from 0.47 to 0.49 (Fig. 4; Supplementary Table S3).

All studied metabasalts contain common accessory minerals: apatite, rutile, ilmenite and magnetite.

*Zlatník Formation metabasalts*: The prevalent part of the Zlatník metabasalts are fine-grained with well-developed schistosity and microfolds. Due to the generally occurring fine-grained texture, we assume the originally aphanitic texture to be predominant in these metabasalts (Figs. 2C,D). Relics of microporphyric textures were revealed. Rare porphyric crystals of plagioclases were completely saussuritized. Due to distinct metamorphic overprint, the rocks are composed of very fine-grained crystalline aggregate of chlorite, epidote/zoizite, albite, white mica, calcite, Fe–Ti oxides, titanite and quartz (in approximate order of abundance).

The chemical composition of the white micas is linked to the muscovite–celadonite series (after Tischendorf et al. 2007; Fig. 5), containing a higher amount of tetrahedral co-ordinated Si, in the range from 3.3 to 3.6 *a.p.f.u.*, as well as a high amount of Mg and Fe in octahedral M site (Supplementary Table S4). The white mica is enriched with a celadonite component ($Fe^{+2}$ to 0.36 *a.p.f.u.* and $Mg^{+2}$ to 0.39 *a.p.f.u.*), which is indicated by the shift from the ideal muscovite to the phengite field. Muscovite with a higher content of $Cr_2O_3$ (5.85 w. %, analysis no. 8) was rarely found in the sample *GZ-49*. The content of other cations is low, with the exception of Na (0.16 *a.p.f.u.* in analysis no. 10) in sample *GZ-49*.

Chlorites, which are the most abundant mineral in metabasalts, belong mainly to the Mg-chlorite (Clinochlore) group (after Zane & Weiss 1998) due to their composition (Fig. 4; Supplementary Table S3), with the magnesium number *mg#* in the range from 0.48 to 0.63, with the average value 0.55. The content of other cations is negligible or zero, with the exception of Mn, with a content not exceeding 0.03 *a.p.f.u.*

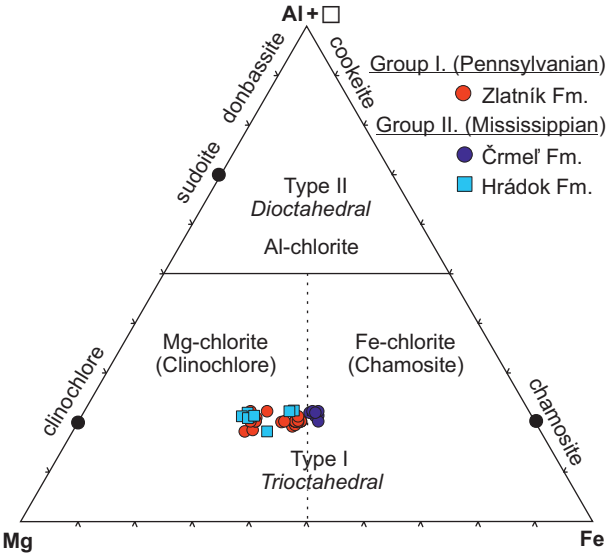


**Fig. 4.** Classification diagram of chlorites (according to Zane & Weiss 1998).

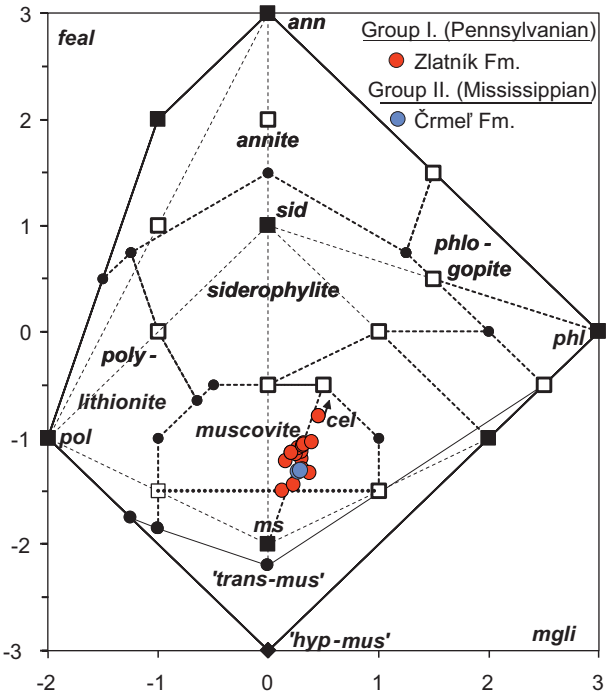


**Fig. 5.** Classification ***mgfli/feal*** diagram of white micas (according to Tischendorf et al. 2007).

### *Metamorphic constrains*

The temperature-pressure conditions of metamorphic recrystallization were estimated on the basis of a chlorite geothermometers (after Cathelineau 1988; Jowett 1991) and multi-reaction equilibria geothermobarometry (Vidal et al. 2006).

*Hrádok Formation:* Unfortunately, there is no phengite present in the Hrádok Fm., so it was not possible to use the barometry of Vidal et al. (2006). However, Chl–Qtz–$H_2O$ thermometry yield temperatures of 274–345 °C. Comparable temperatures were obtained by Chlorite-thermometry of Cathelineau (1988) and Jowett (1991) in the interval between 240–356 °C and 245–359 °C, respectively (Fig. 6).

*Črmeľ Formation:* According to Vidal et al. (2006) multi-equilibria geothermobarometry, the Črmeľ Formation underwent temperatures around 295–337 °C and pressures of 0.6–0.8 GPa (Fig. 7A). Moderately higher temperatures with

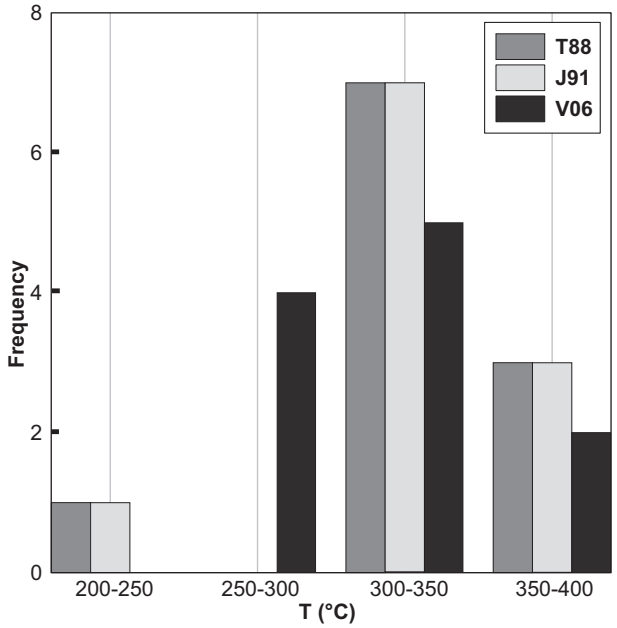


**Fig. 6.** Temperature estimations for the Hrádok Fm. based on chlorite thermometry (after Cathelineau 1988 (*T88*); Jowett 1991 (*J91*); and Vidal 2006 (*V06*).

narrower interval were obtained by Chl-thermometry of Cathelineau (1988) of 325–340 °C and Jowett (1991) 331–358 °C (Fig. 7B).

*Zlatník Formation:* In Zlatník Fm. metabasites, Chl–Ph–Qtz–$H_2O$ multi-equilibria geothermobarometry (Vidal et al. 2006) shows pressures 0.4–0.6 GPa at temperatures 274–345 °C (Fig. 8A). Chlorite-thermometry of Cathelineau (1988) and Jowett (1991) shows temperatures with a comparable interval between 278–356 °C and 359–380 °C, respectively (Fig. 8B).

There is no doubt that the associations of metamorphic minerals found in the Pennsylvanian and Mississippian NGU metabasites correspond to the temperature–pressure conditions of the greenschist facies. Both the chemical compositions of index metamorphic minerals and the results of geothermobarometric recalculations link to the greenschist facies (Table 2; Figs. 6–8). The presented geothermobarometric calculations show that no differences were found between these three studied groups of metabasites in the temperature conditions of regional metamorphosis, generally maxima in the range of 300–350 °C. Smaller differences are observed in the pressures, when for the Pennsylvanian Zlatník Fm. lower pressures (0.4–0.6 GPa) were calculated compared to the Mississippian Črmeľ Fm. (0.6–0.8 GPa).

However, there is a certain difference in the representation of index metamorphic minerals. Two groups of metamorphic assemblages were distinguished among the studied metabasites, the first Act-absent with presence of Chl+Ab+Ep±Ms, Ttn, Qtz, Cal (the Pennsylvanian Zlatník Fm.) and the second Act-bearing accompanied by Chl+Ab+Ep±Ttn, Qtz and scarce muscovite (the Mississippian Hrádok and Črmeľ fms.). The absence of Act in the metamorphic community of metabasites in the Zlatník Fm. suggests that P–T conditions corresponded first to the transition between sub-greenschist and greenschist facies. In the presence of $CO_2$ fluids, which indicates the abundance of calcite, the Chl+Ep association may occur even at lower temperatures, below 300 °C (Bucher & Grapes 2011 and references therein).

### *Geochemistry*

Immobile trace elements such as high field strength elements (HFSE) and rare elements (REEs) have been used to classify rocks and monitor magmatic affinities. Representative major- and trace elements including REEs are given in Table 3. All fifteen analysed volcanic rocks belong mostly to the group of basalts and fewer to the andesite-basalts of the subalkaline magmatic series according to the Zr/Ti versus Nb/Y classification (based on Winchester & Floyd 1977; revised by Pearce 1996, 2014) (Fig. 9A). This is clearly documented by Nb/Y ratios ranging from 0.03 to 0.21 (<1; Pearce 1982). Carboniferous metabasalts to meta-andesites of the NGU zone belong to the low-Ti tholeiitic series, which is characterized by the $TiO_2$ contents of less than 2.5 % and the Ti/Y ratios below 500. However, within the Pennsylvanian (Group I) and Mississippian (Group II) volcanics, slight differences were observed. The volcanic rocks of the Group I are all concentrated near the andesite-basalts/basalts discriminant line. Although the $SiO_2$ contents do not differ (Table 3), the Group I metabasalts have higher contents of $Al_2O_3$ (15.33–17.10 wt. %), $Na_2O$ (3.45–4.36 wt. %), $K_2O$ (0.49–1.83 wt. %), $TiO_2$ (1.48–2.06 wt. %) and lower contents of MgO (4.00–6.41 wt. %). High contents of LOI (4.9–10.7 wt. %) are caused by a relatively higher calcite content in their texture that originated in the conditions of sub-greenschist / greenschists facies, especially at the expense of magmatic plagioclases and Mg–Fe silicates.

Compared to these, the metabasalts of Group II are characterized by a narrow range of $Al_2O_3$ (13.71–15.81 wt. %), $Na_2O$ (2.08–3.19 wt. %) and $K_2O$ (0.08–0.30 wt. %), and variable contents of MgO (6.21–12.10 wt. %), CaO (6.21–12.10 wt. %) and $TiO_2$ (0.48–2.24 wt. %). The *Mg #* [molar 100 MgO/(MgO+FeO)] values also vary accordingly, ranging from 44 to 59 in the Group I metabasalts and 50 to 58 in the Group II metabasalts. The compositional diversity of the studied metabasalts is further emphasized by other elemental ratios. These rocks also have differences in Ti/V (35.2–49.9 in Group I and 15.5–42.7 in Group II), Zr/Nb (31.6–87.5 in Group I and 13.3–24.6 in Group II), Zr/Y (2.97–5.05 versus 1.17–4.19), Nb/Yb (0.36–1.63 versus 0.75–3.79) and La/Nb (2.03–4.08 versus 1.07–1.5).

An exception is the *GZ-43* sample from Group II, which chemically corresponds to meta-andesites. In addition to $SiO_2$ (56.26 wt. %), of course, this rock compared to metabasalts, has increased content of $Na_2O$ (5.08 wt.%) and a reduced content of MgO (2.79 wt. %) and CaO (3.90 wt. %), as well as substantially lower *mg#* values (34.5). Of the trace

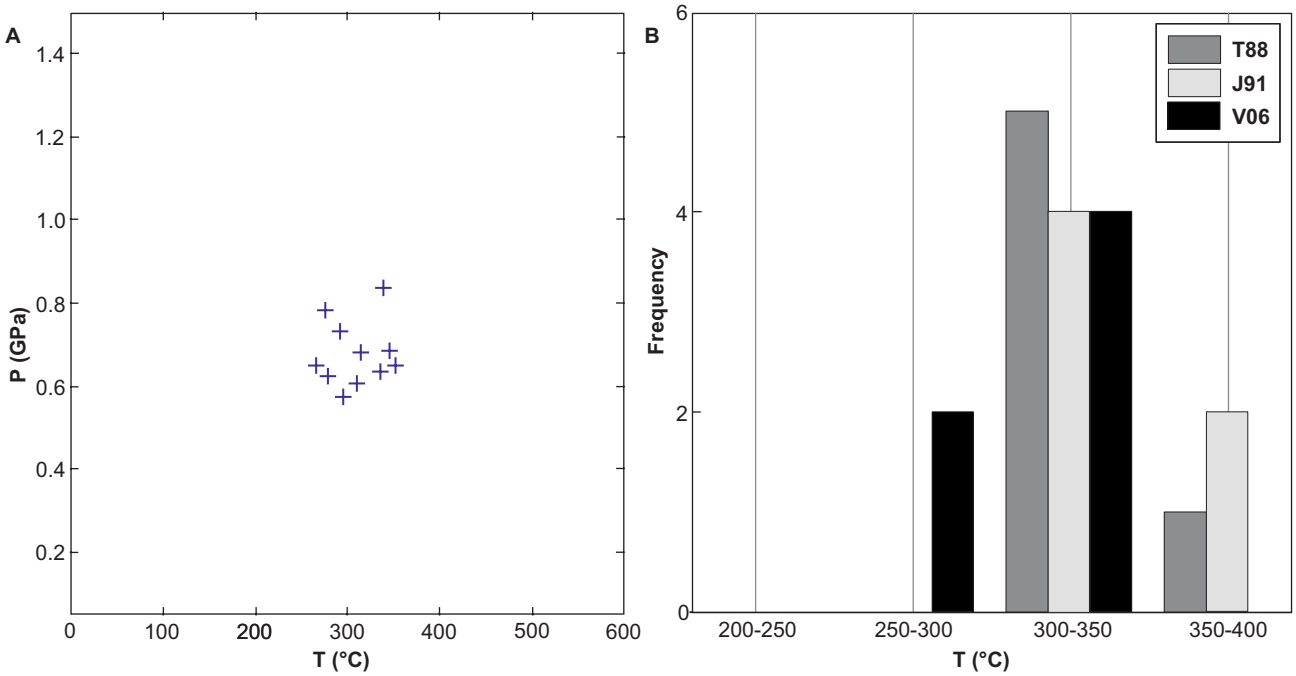


**Fig. 7.** Temperature–pressure estimations for the Črmeľ Fm.; metamorphic recrystallization estimated on the basis: **A** — multiequilibria geothermobarometry (Vidal et al. 2006); **B** — chlorite geothermometer see explanation to Fig. 6.

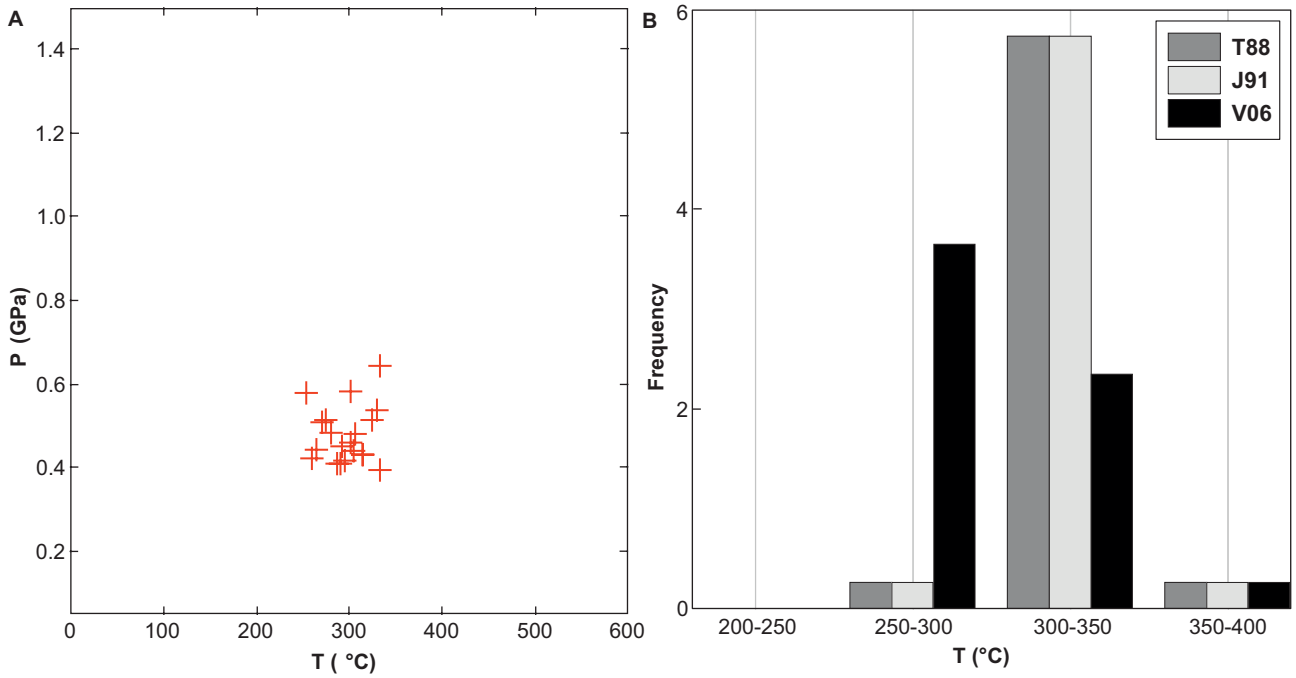


**Fig. 8.** Temperature–pressure estimations for the Zlatník Fm.; metamorphic recrystallization estimated on the basis: **A** — multi-equilibria geothermobarometry (Vidal et al. 2006); **B** — chlorite geothermometer chlorite see explanation to Fig. 6.

elements, it shows higher contents of Hf, Nb, Sr, Th, Zr and Y.

Relatively larger differences were found between these two groups of metabasalts in the total REE content. Although the total REE content in the studied metabasalts is low to moderate, differences between metabasalts I and II were nevertheless found. If the Group I metabasalts contain on average 73.98 ppm (n=5) of REE, the Group II metabasalts have only 51.69 ppm (n=9). Distribution of the chondrite normalized REE curves (after McDonough & Sun 1995) show

**Table 2:** Results of chlorite geothermometric recalculations after Cathelineau 1988 (*TC88*), Jowett 1991 (*TJ91*) and Vidal et al. 2006 (*TV06*).

| Sample | Mineral | An. N.: | *TC88* (°C) | *TJ91* (°C) | *V06* (°C) |
|---|---|---|---|---|---|
| **Tectonic U.: Zlatník Formation (Pennsylvanian)** | | | | | |
| *GZ-49* | Chl | 2 | 317 | 320 | 300 |
| *GZ-49* | Chl | 4 | 307 | 309 | 309 |
| *GZ-49* | Chl | 7 | 278 | 280 | 285 |
| *GZ-53* | Chl | 1 | 323 | 328 | 288 |
| *GZ-53* | Chl | 2 | 302 | 306 | 278 |
| *GZ-53* | Chl | 3 | 311 | 316 | 289 |
| *GZ-53* | Chl | 4 | 302 | 307 | 284 |
| *GZ-53* | Chl | 5 | 316 | 321 | 292 |
| *GZ-54* | Chl | 2 | 317 | 319 | 299 |
| *GZ-54* | Chl | 5 | 309 | 311 | 312 |
| *GZ-54* | Chl | 6 | 306 | 308 | 298 |
| *GZ-53* | Chl | 2 | 323 | 328 | 296 |
| *GZ-53* | Chl | 4 | 320 | 325 | 321 |
| *GZ-53* | Chl | 5 | 310 | 314 | 293 |
| *GZ-53* | Chl | 8 | 316 | 320 | 288 |
| *GZ-53* | Chl | 9 | 337 | 342 | 398 |
| *GZ-53* | Chl | 10 | 312 | 317 | 308 |
| *GZ-53* | Chl | 11 | 343 | 348 | 288 |
| *GZ-53* | Chl | 12 | 334 | 339 | 327 |
| *GZ-53* | Chl | 14 | 329 | 334 | 311 |
| *GZ-54* | Chl | 2 | 311 | 312 | 287 |
| *GZ-54* | Chl | 3 | 342 | 343 | 340 |
| *GZ-54* | Chl | 4 | 356 | 359 | 291 |
| *GZ-54* | Chl | 5 | 332 | 334 | 319 |
| **Tectonic U.: Hrádok Formation (Mississippian)** | | | | | |
| *GZ-51* | Chl | 2 | 322 | 323 | 301 |
| *GZ-41a* | Chl | 8 | 240 | 243 | 277 |
| *GZ-52* | Chl | 7 | 352 | 356 | 354 |
| *GZ-51* | Chl | 1 | 317 | 318 | 287 |
| *GZ-51* | Chl | 3 | 311 | 311 | 299 |
| *GZ-51* | Chl | 4 | 338 | 338 | 330 |
| *GZ-51* | Chl | 9 | 324 | 325 | 329 |
| *GZ-51* | Chl | 10 | 356 | 357 | 343 |
| *GZ-51* | Chl | 15 | 346 | 347 | 304 |
| *GZ-52* | Chl | 1 | 344 | 348 | 299 |
| *GZ-52* | Chl | 4 | 355 | 359 | 355 |
| **Tectonic U.: Črmeľ Formation (Mississippian)** | | | | | |
| *GZ-42* | Chl | 5 | 345 | 350 | 316 |
| *GZ-42* | Chl | 7 | 331 | 336 | 299 |
| *GZ-43* | Chl | 4 | 325 | 331 | 306 |
| *GZ-45* | Chl | 4 | 345 | 351 | 337 |
| *GZ-42* | Chl | 2 | 340 | 346 | 318 |
| *GZ-42* | Chl | 4 | 353 | 358 | 321 |

an almost identical flat course, with low LREE enrichment with no or only weak positive or negative Eu anomaly (Fig. 9B). The *Eu/Eu** values vary between 0.88 and 1.23 (mean 1.05±0.16, n=5) within the Group I metabasalts and between 0.89 and 1.17 within the Group II metabasalts (mean 1.01±0.08, n=9) (Table 3). The evident positive anomaly in the majority of samples attests to some minor plagioclase accumulation in the fractionated mineral assemblages. An exception is the *GZ-51* sample, which is extremely depleted of REE (∑REE=30.76 ppm) and additionally depleted of Ta, Th, U, Nb. The course of normalized contents of REE elements is approximately the same in the studied metabasalts on the heavy REE (HREE) side. The degree of enrichment/depletion of LREE expressed by the ratio $(La/Sm)_N$ is low and varies in the range of 0.71 to 1.42 in the Group I and from 0.90 to 1.40 in the Group II. Only the *GZ-51* sample is different, where a significant depletion of LREE is observed, $(La/Sm)_N$=0.43. The $(La/Yb)_N$ ratios also indicate a relatively low LREE enrichment: from 0.99 to 2.76 in the Group I metabasalts and from 0.41 to 2.77 for the Group II metabasalts.

An exception is the *GZ-43* meta-andesite sample, which shows several times higher REE contents (∑REE=195.56 ppm) compared to metabasalts, while the LREE enrichment is evidently higher, $(La/Sm)_N$=3.41 and $(La/Yb)_N$=3.92.

A week fractionation of medium REE (MREE) to HREE in all studied metabasalt samples is indicative, as well as the depletion in HREE with respect to MREE. In fact, the $(Sm/Yb)_N$ ratios are higher than that of typical N-MORB ($Sm_N/Yb_N$)=0.96; Sun & McDonough 1989), as they range from 1.43 to 1.98 in the Group I and from 0.86 to 2.05 in the Group II metabasalts. It should be noted that Group II metabasalts have a higher variability $(Sm/Yb)_N$ ratios than Group I metabasalts. However, samples with a higher value of $(Sm/Yb)_N$ ratios are dominant, and only three samples show values <1 which are typical for N- MORB.

Spider diagrams (normalized to primitive mantle after Sun & McDonough 1989) show partly similar enrichment and depletion trends (Fig. 9C). Distinct negative Ba, Th, U, Ta, Nb and week Ti anomalies and positive anomalies of Cs, Rb, K and Pb were observed in Group I metabasalts. In all samples of the Group I metabasalts, a slight depletion of HREE was observed, as shown by the decreasing trend in the direction from Gd to Lu (Fig. 9C). In Group II metabasalts the trend is similar, negative anomalies for Rb, Ba, Th, Ta, Sr, except to observed depletion of K. The trend of depletion of HREE is slightly more pronounced than for metabasalts of Group I. The *GZ-51* sample, compared to other metabasalts of Group II, is characterized by relatively depletion of Ta, Nb, P, Ti, Sr, Zr and LREE. An isolated sample of andesite (*GZ-43*) shows enrichment in all REE, Cs, Th, U, and Zr and depletion of K and Ti.

### *Isotope composition*

The Sm–Nd isotopic data together with Sr isotopic analyses are listed in Table 4. With the exception of the sample *GZ-43* (meta-andesite), all analysed samples for Sm–Nd isotopes are metabasalts.

The three Group I metabasalt samples are relatively similar in REE contents (Nd ranging between 13.52 and 16.40 ppm and Sm ranging between 4.22 and 5.12 ppm) and $^{147}Sm/^{144}Nd_{(0)}$ ratios extending from 0.1744 to 0.2003 (Table 4). The measured $^{87}Sr/^{86}Sr_{(0)}$ values vary between 0.7053 and 0.7081 and the $\varepsilon Nd_{(0)}$ flanked by +7.92 and +8.68. The εNd(t) calculated at 320 Ma is also relatively balanced in the range of +8.25 and +8.54 (Table 4).

**Table 3:** Representative major-, trace elements, including REE in the NGU Mississippian and Pennsylvanian metabasalts (n.d. – under detection limit; + twice measured of sample)

| | | Pennsylvanian | | | | | Mississippian | | | | | | | | | |
|---|---|---|---|---|---|---|---|---|---|---|---|---|---|---|---|---|
| | | *GZ49* | *GZ53* | *GZ54* | *GZ11* | *GZ12* | *GZ51* | *GZ51⁺* | *GZ52* | *GZ41A* | *GZ41B* | *GZ18* | *GZ19* | *GZ30* | *GZ42* | *GZ43* | *GZ45* |
| | u | Zlatník Fm. | | | | | Hrádok Fm. | | | Črmeľ Fm. | | | | | | | |
| $SiO_2$ | % | 44.76 | 44.96 | 45.11 | 42.98 | 48.30 | 50.65 | 51.42 | 47.22 | 47.20 | 44.31 | 46.95 | 47.85 | 46.71 | 45.86 | 56.26 | 46.80 |
| $Al_2O_3$ | % | 19.57 | 17.10 | 17.02 | 15.33 | 16.37 | 14.64 | 14.52 | 14.35 | 14.17 | 15.81 | 14.36 | 14.61 | 14.10 | 13.71 | 15.73 | 14.88 |
| $Fe_2O_3$ | % | 9.72 | 9.97 | 8.66 | 9.09 | 10.85 | 8.13 | 8.03 | 11.92 | 14.70 | 13.27 | 13.14 | 11.43 | 13.05 | 13.39 | 10.61 | 11.98 |
| MgO | % | 4.49 | 4.00 | 6.41 | 5.25 | 4.78 | 8.63 | 8.32 | 8.03 | 7.79 | 6.72 | 7.53 | 6.88 | 7.31 | 7.85 | 2.79 | 7.08 |
| CaO | % | 9.63 | 10.88 | 7.46 | 10.31 | 6.00 | 10.99 | 11.38 | 11.33 | 6.21 | 9.82 | 10.54 | 12.10 | 11.64 | 11.39 | 3.90 | 10.75 |
| $Na_2O$ | % | 3.57 | 3.79 | 4.36 | 3.45 | 3.52 | 3.19 | 3.27 | 2.09 | 4.25 | 2.57 | 2.10 | 2.08 | 2.19 | 2.15 | 5.08 | 2.84 |
| $K_2O$ | % | 1.35 | 0.48 | 0.63 | 0.77 | 1.83 | 0.11 | 0.11 | 0.08 | 0.25 | 0.27 | 0.27 | 0.30 | 0.06 | 0.15 | 0.16 | 0.27 |
| $TiO_2$ | % | 1.48 | 1.86 | 1.93 | 1.64 | 2.06 | 0.48 | 0.45 | 1.42 | 1.44 | 2.24 | 1.55 | 1.49 | 1.61 | 1.85 | 1.61 | 1.48 |
| $P_2O_5$ | % | 0.13 | 0.19 | 0.19 | 0.19 | 0.24 | 0.02 | 0.04 | 0.10 | 0.14 | 0.22 | 0.13 | 0.09 | 0.15 | 0.16 | 0.30 | 0.13 |
| MnO | % | 0.11 | 0.14 | 0.12 | 0.14 | 0.15 | 0.15 | 0.15 | 0.17 | 0.19 | 0.15 | 0.18 | 0.18 | 0.20 | 0.20 | 0.13 | 0.18 |
| $Cr_2O_3$ | % | 0.033 | 0.028 | 0.028 | 0.028 | 0.032 | 0.017 | 0.019 | 0.038 | 0.014 | 0.014 | 0.022 | 0.037 | 0.05 | 0.041 | 0.005 | 0.032 |
| LOI | % | 4.9 | 6.4 | 7.9 | 10.7 | 5.7 | 2.8 | 2.2 | 3.0 | 3.5 | 4.4 | 3.0 | 2.7 | 2.7 | 3.1 | 3.2 | 3.4 |
| Ba | ppm | 75 | 19 | 34 | 65 | 67 | 19 | 23 | 14 | 38 | 54 | 70 | 59 | 23 | 42 | 97 | 75 |
| Ni | ppm | 83 | 62 | 63 | 69 | 75 | 126 | 103 | 76 | 58 | 95 | 79 | 99 | 95 | 93 | 24 | 77 |
| Sc | ppm | 32 | 36 | 33 | 29 | 37 | 47 | 50 | 41 | 46 | 42 | 45 | 49 | 46 | 44 | 21 | 41 |
| Sum | % | 99.79 | 99.81 | 99.80 | 99.84 | 99.83 | 99.78 | 99.89 | 99.71 | 99.85 | 99.82 | 99.75 | 99.80 | 99.81 | 99.82 | 99.77 | 99.84 |
| Cs | ppm | 2.3 | 0.5 | 1.2 | 1.8 | 2.3 | n.d. | n.d. | n.d. | 1.2 | 0.3 | 0.3 | 0.6 | 0.1 | n.d. | 0.3 | 0.3 |
| Ga | ppm | 19.2 | 16.6 | 16.2 | 14.1 | 17.4 | 13.9 | 14.5 | 16.5 | 17.7 | 18.2 | 18.7 | 19.2 | 19.6 | 17.1 | 22.8 | 17.6 |
| Hf | ppm | 2.7 | 3.6 | 3.3 | 3.5 | 4.4 | 1.0 | 1.0 | 2.1 | 2.8 | 3.5 | 2.4 | 2.2 | 2.4 | 2.8 | 9.3 | 1.8 |
| Nb | ppm | 1.2 | 2.6 | 3.3 | 4.2 | 3.9 | n.d. | 0.4 | 4.9 | 3.4 | 9.3 | 6.2 | 4.8 | 5.4 | 5.9 | 8.1 | 4.6 |
| Rb | ppm | 36.1 | 10.7 | 17.2 | 28.5 | 43.4 | 1.2 | 1.0 | 1.4 | 5.9 | 3.6 | 7.2 | 9.8 | 0.8 | 2.0 | 4.2 | 4.5 |
| Sr | ppm | 366.8 | 268.9 | 86.8 | 129.0 | 143.2 | 155.7 | 152.1 | 457.6 | 104.7 | 224.9 | 249.3 | 136.5 | 444.5 | 335.1 | 594.8 | 284.1 |
| Ta | ppm | 0.2 | 0.1 | 0.2 | 0.1 | 0.3 | n.d. | n.d. | 0.3 | 0.1 | 0.6 | 0.3 | 0.3 | 0.4 | 0.5 | 0.5 | 0.3 |
| Th | ppm | 0.2 | 0.3 | 0.3 | 1.9 | 1.2 | n.d. | n.d. | 0.4 | 0.2 | 0.6 | 1.1 | 1.4 | 0.3 | 0.4 | 5.1 | 0.2 |
| U | ppm | n.d. | 0.1 | 0.3 | 0.5 | 0.4 | n.d. | n.d. | 0.1 | 0.2 | 0.1 | 0.3 | 0.2 | n.d. | n.d. | 1.7 | n.d. |
| V | ppm | 252 | 278 | 248 | 197 | 255 | 185 | 187 | 306 | 389 | 314 | 334 | 341 | 333 | 354 | 115 | 287 |
| Zr | ppm | 105.0 | 143.5 | 139.0 | 132.7 | 165.5 | 26.8 | 30.3 | 82.1 | 83.6 | 124.2 | 84.9 | 73.6 | 84.9 | 98.5 | 429.4 | 77.1 |
| Y | ppm | 35.3 | 33.2 | 27.5 | 27.6 | 40.6 | 22.9 | 24.3 | 23.3 | 43.2 | 29.6 | 27.2 | 22.6 | 26.5 | 27.9 | 58.1 | 22.3 |
| La | ppm | 4.9 | 5.8 | 6.7 | 10.5 | 8.7 | 1.5 | 1.6 | 5.8 | 5.1 | 10.0 | 6.7 | 6.6 | 6.4 | 8.3 | 32.0 | 5.0 |
| Ce | ppm | 13.1 | 16.3 | 18.6 | 25.1 | 22.1 | 4.3 | 4.6 | 13.2 | 13.4 | 25.1 | 16.7 | 14.2 | 16.0 | 18.9 | 65.9 | 13.7 |
| Pr | ppm | 2.36 | 2.74 | 2.99 | 3.86 | 3.79 | 0.82 | 0.83 | 2.19 | 2.02 | 3.59 | 2.56 | 2.32 | 2.25 | 2.93 | 9.19 | 2.09 |
| Nd | ppm | 12.2 | 14.4 | 15.5 | 18.0 | 19.5 | 5.8 | 5.5 | 10.0 | 11.0 | 17.1 | 11.7 | 11.6 | 10.9 | 12.7 | 38.6 | 10.7 |
| Sm | ppm | 4.29 | 4.53 | 4.78 | 4.6 | 5.53 | 2.19 | 1.97 | 3.17 | 3.54 | 4.53 | 3.56 | 2.94 | 3.44 | 3.97 | 9.38 | 2.73 |
| Eu | ppm | 2.04 | 1.69 | 1.53 | 1.93 | 1.76 | 0.89 | 1.00 | 1.21 | 1.44 | 1.48 | 1.26 | 1.27 | 1.35 | 1.58 | 2.78 | 1.06 |
| Gd | ppm | 5.93 | 6.07 | 5.06 | 5.17 | 6.67 | 3.42 | 3.30 | 4.34 | 5.75 | 5.63 | 4.40 | 3.57 | 4.53 | 5.09 | 10.13 | 3.97 |
| Tb | ppm | 1.03 | 1.05 | 0.92 | 0.94 | 1.23 | 0.66 | 0.61 | 0.73 | 0.93 | 0.85 | 0.82 | 0.69 | 0.70 | 0.81 | 1.57 | 0.61 |
| Dy | ppm | 6.38 | 6.20 | 5.57 | 5.25 | 7.32 | 4.38 | 4.27 | 4.40 | 7.60 | 6.07 | 4.83 | 3.90 | 5.72 | 5.62 | 10.83 | 4.77 |
| Ho | ppm | 1.38 | 1.27 | 1.14 | 1.02 | 1.50 | 0.89 | 0.90 | 0.92 | 1.52 | 1.10 | 1.01 | 0.85 | 0.97 | 0.99 | 2.11 | 0.81 |
| Er | ppm | 3.82 | 3.63 | 3.20 | 2.86 | 4.40 | 2.65 | 2.82 | 2.63 | 4.34 | 2.89 | 2.98 | 2.60 | 2.62 | 2.82 | 5.81 | 2.32 |
| Tm | ppm | 0.52 | 0.52 | 0.45 | 0.44 | 0.68 | 0.41 | 0.38 | 0.35 | 0.67 | 0.40 | 0.43 | 0.37 | 0.39 | 0.41 | 0.85 | 0.33 |
| Yb | ppm | 3.33 | 3.25 | 2.86 | 2.58 | 4.02 | 2.46 | 2.54 | 2.32 | 4.51 | 2.45 | 2.70 | 2.27 | 2.46 | 2.59 | 5.54 | 2.05 |
| Lu | ppm | 0.49 | 0.50 | 0.44 | 0.40 | 0.59 | 0.39 | 0.36 | 0.35 | 0.72 | 0.37 | 0.39 | 0.31 | 0.37 | 0.42 | 0.87 | 0.33 |
| Pb | ppm | 4.2 | 2.7 | 2.6 | 1.4 | 2.2 | 1.7 | n.d. | 2.7 | 1.1 | 1.2 | 1.5 | 1.5 | 0.6 | 0.8 | 3.8 | 0.9 |
| TOT/C | % | 0.40 | 0.99 | 1.09 | 2.05 | 0.52 | 0.12 | 0.15 | 0.02 | 0.16 | n.d. | n.d. | 0.47 | 0.03 | n.d. | 0.15 | 0.17 |
| TOT/S | % | n.d. | n.d. | n.d. | n.d. | n.d. | n.d. | n.d. | n.d. | n.d. | n.d. | n.d. | n.d. | n.d. | n.d. | n.d. | n.d. |
| Eu/Eu* | | 1.233 | 0.982 | 0.948 | 1.206 | 0.883 | 0.991 | 1.196 | 0.994 | 0.973 | 0.893 | 0.970 | 1.195 | 1.042 | 1.071 | 0.869 | 0.981 |
| $(Ta/La)_{PM}$ | | 0.684 | 0.289 | 0.500 | 0.160 | 0.578 | 0.000 | 0.000 | 0.867 | 0.329 | 1.005 | 0.750 | 0.762 | 1.047 | 1.009 | 0.262 | 1.005 |
| $(Hf/Sm)_{PM}$ | | 0.904 | 1.142 | 0.992 | 1.093 | 1.143 | 0.656 | 0.729 | 0.952 | 1.137 | 1.110 | 0.969 | 1.075 | 1.002 | 1.013 | 1.425 | 0.947 |

Among the Group II metabasalts, the three samples are similar in REE content (Nd ranging between 11.8 and 14.2 ppm and Sm ranging between 3.65 and 4.26 ppm) as well as in relatively uniform $^{147}Sm/^{144}Nd_{(0)}$ ratios, ranging from 0.1807 to 0.1866. The *GZ-51* metabasalt sample was collected in proximity at the sheared tectonic contact with the Veporic Unit and shows depletion of Nd and Sm (6.7 and 2.66, respectively) and, conversely, a higher $^{147}Sm/^{144}Nd_{(0)}$ ratio (0.2402). This metabasalt has a medium-grained texture with evidence of dynamic recrystallization of amphibole and plagioclase porphyroblasts and thus isotopic disequilibrium could have been produced. The *GZ-43* meta-andesite sample has increased REE contents compared to metabasalts (Nd 36.7 and Sm 8.71 ppm) and, conversely, a lower $^{147}Sm/^{144}Nd_{(0)}$ ratio,

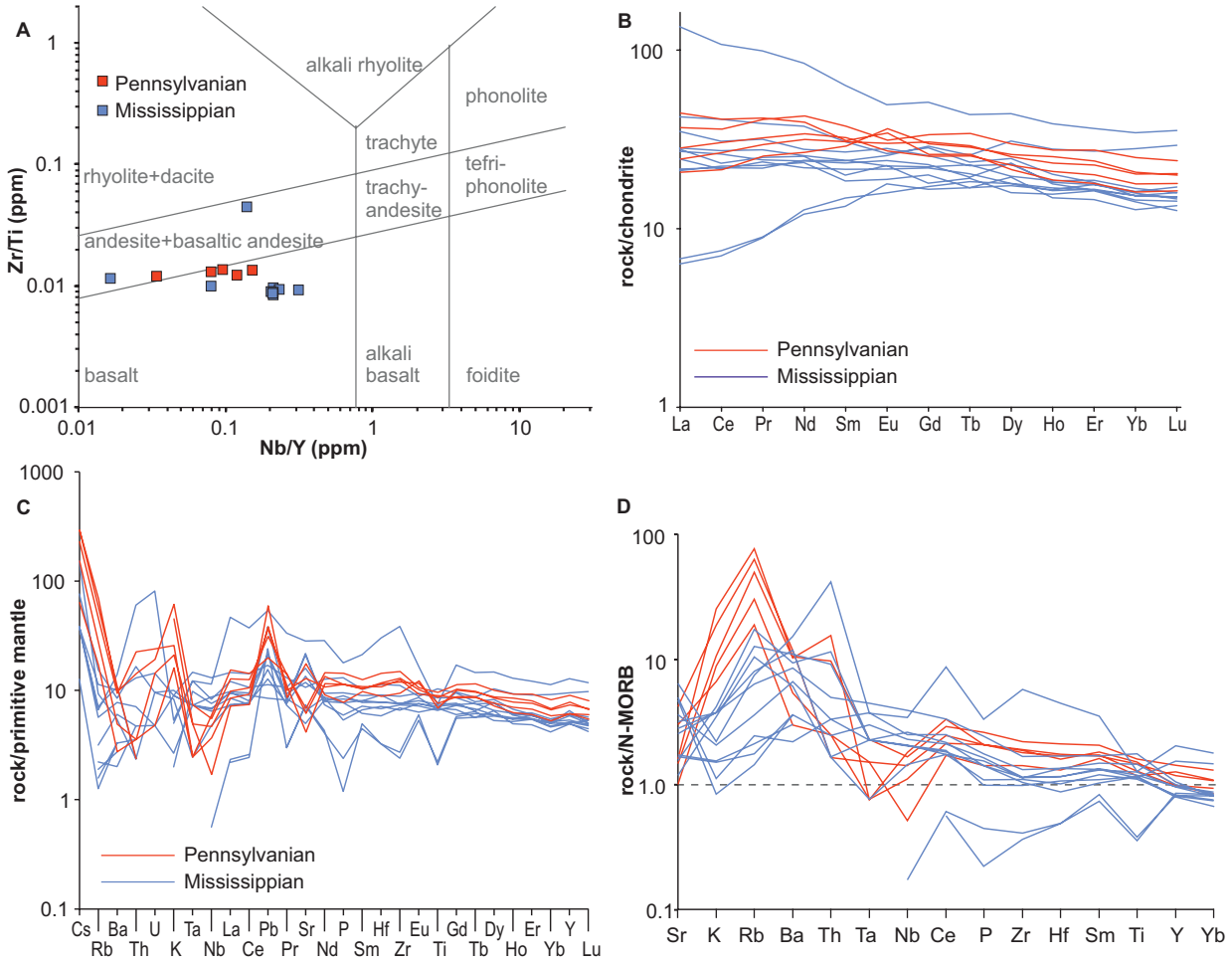


**Fig. 9. A** — Distribution of the SGU metavolcanic rocks based on Zr/Ti versus Nb/Y after Pearce (1996) diagram (revised Winchester & Floyd 1977); **B** — Chondrite normalized REE distribution of the studied samples. Chondrite normalizing values after McDonough & Sun (1995); **C** — Primitive mantle normalized incompatible element's diagram of the studied samples. Normalizing values after Sun & McDonough (1989); **D** — N-MORB normalized incompatible element's diagram of the studied samples. Normalizing values after Sun & McDonough (1989).

**Table 4:** Sr and Nd analysis data of the Mississippian and Pennsylvanian NGU metavolcanic rocks, calculated for emplacement time T=340 and 320 Ma. $T_{(DM)}$: *D after DePaolo (1981), *LH after Liew & Hofmann (1988). Uncertainties given at 2sigma m level.

| Sample | t (Ma) | $^{147}Sm/^{144}Nd_{(0)}$ | $^{143}Nd/^{144}Nd_{(0)}$ | 2σ | $^{87}Sr/^{86}Sr_{(0)}$ | 2σ | $T_{DM*D}$ (Ga) | $T_{DM*2st-LH}$ (Ga) | $\varepsilon Nd_{(0)}$ | $\varepsilon Nd_{(t)}$ |
|---|---|---|---|---|---|---|---|---|---|---|
| *Pennsylvanian* | | | | | | | | | | |
| *GZ-49* | 320 | 0.2003 | 0.513083 | 0.000004 | 0.708164 | 0.000011 | 0.55 | 0.36 | 8.68 | 8.54 |
| *GZ-53* | 320 | 0.1888 | 0.513044 | 0.000009 | 0.705341 | 0.000009 | 0.54 | 0.39 | 7.92 | 8.25 |
| *GZ-54* | 320 | 0.1744 | 0.513022 | 0.000007 | 0.708087 | 0.000014 | 0.44 | 0.37 | 7.49 | 8.41 |
| *Mississippian* | | | | | | | | | | |
| *GZ-42* | 340 | 0.1813 | 0.512873 | 0.000009 | 0.705246 | 0.000013 | 1.12 | 0.64 | 4.59 | 5.27 |
| *GZ-43* | 340 | 0.1439 | 0.512673 | 0.000007 | 0.710993 | 0.000008 | 0.97 | 0.82 | 0.68 | 2.98 |
| *GZ-45* | 340 | 0.1866 | 0.512951 | 0.000009 | 0.706094 | 0.000011 | 0.94 | 0.54 | 6.11 | 6.56 |
| *GZ-51* | 340 | 0.2402 | 0.513177 | 0.000009 | 0.705663 | 0.000010 | 0.19 | 0.37 | 10.52 | 8.64 |
| *GZ-52* | 340 | 0.1807 | 0.512918 | 0.000009 | 0.707639 | 0.000013 | 0.93 | 0.57 | 5.46 | 6.17 |

corresponding to 0.1495 as expected. Compared to Group I metabasalts, the $\varepsilon Nd_{(0)}$ values for Group II metabasalts are variable, ranging from +4.59 to +10.52 for metabasalts and +0.68 for meta-andesite. The calculated εNd(t) values for all Group II metavolcanic samples vary on a larger scale, from +5.27 to +8.64 for metabasalts and +2.98 for meta-andesite (Table 4).

However, in the $^{143}Nd/^{144}Nd_{(0)}$ vs. $^{87}Sr/^{86}Sr_{(0)}$ diagram, the projection points of both groups of metabasites appear instead of the quadrant I indicating the depleted mantle source,

in the quadrant II (according to Faure 1986), to the right of the mantle array (Fig. 10A). An almost linear trend can be observed on the $^{143}Nd/^{144}Nd_{(0)}$ vs. $^{147}Sm/^{144}Nd_{(0)}$ isotope correlation diagram (Fig. 10B) with reference lines for calculated model ages of 355 Ma and 788 Ma, respectively. The $^{147}Sm/^{143}Nd$ isotope ratios in the studied metabasalt samples document a process of Nd enrichment comparing to the CHUR standard (Chondrite Uniform Reservoir; DePaulo & Wasserburg 1976; Wasserburg et al. 1981; DePaulo 1988). This is recognized by the positive values of ε-notation recalculated to time 320 (Group I) and 340 Ma (Group II), respectively (Fig. 10C,D).

## Discussion

The compositional diversity of the studied rocks is conspicuous on the Zr/Ti vs. Nb/Y diagram (Fig. 9A) and is further emphasized by other elemental ratios. Generally, prevailing part of them plot in the basalt field and only a minor part is just below the basaltic andesite/basalt discriminant line or straddling it. Values of Nb/Y for all the Carboniferous metabasic rocks (0.03–0.15 and 0.08–0.31, respectively) denote subalkaline affinities. Also, based on V/Ti values (after Shervais 1982), the majority of studied metabasites fall into the MORB-BABB-CAB field together (Fig. 11). However, on the basis of petrological and chemical signatures, the NGU Carboniferous metabasites may be ascribed to two groups. Coincidentally, their geological position supported by biostratigraphic data (Bouček & Přibyl 1960; Kozur & Mock 1977; Snopková 1978a,b; Bajaník & Planderová 1985) confirmed in the surrounding sediments approves the separation of the Group I (Pennsylvanian) from the Group II (Mississippian) metabasalts. The Group I metabasalts, on the primitive-mantle and N-MORB normalized multi-element diagram (Fig. 9C,D), display higher contents of Zr, Th, Rb and U, Pb, Zn, Ni compared to the metabasalts of the Group II and conversely slightly lower contents of Nb, Ta and V.

Distinct LREE depletion is shown on the basis of $(La/Sm)_N$ ratios (mean 0.96±0.28 for Group I and 1.11±0.32 for Group II)

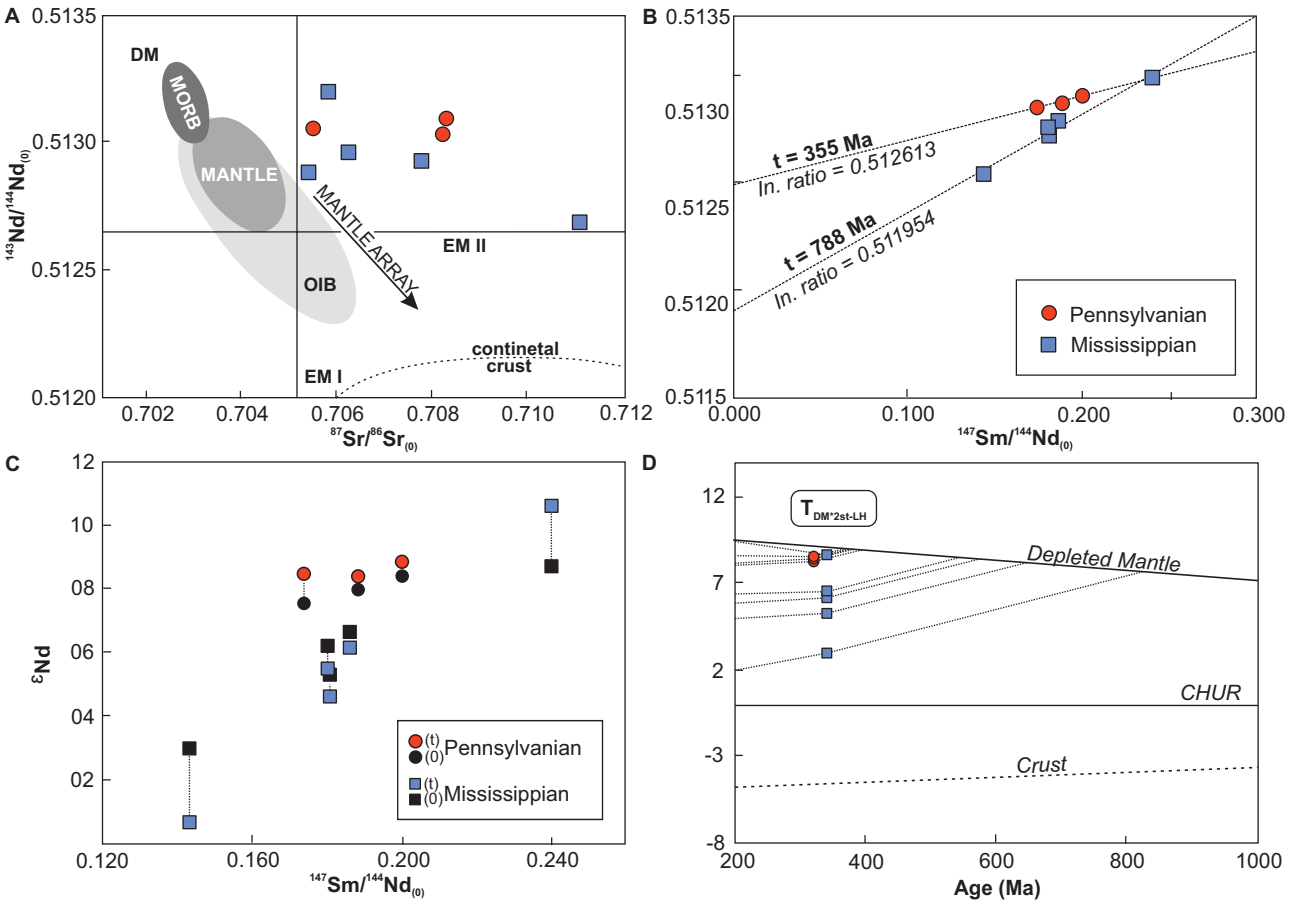


**Fig. 10.** Variation whole-rocks isotope diagrams of NGU metavolcanic rocks. **A** — Diagram $^{143}Nd/^{144}Nd_{(0)}$ vs. $^{87}Sr/^{86}Sr_{(0)}$. *Abbreviations*: DM – Depleted mantle, MORB – Mid Ocean Ridge Basalts, OIB – Ocean Island Basalts (modified after Wilson 1989; Best & Christiansen 2000); EMI – component of Enriched Mantle with a low Sm/Nd ratio leading to low $^{143}Nd/^{144}Nd$; EMII – component of Enriched Mantle with high Rb/Sr and $^{87}Sr/^{86}Sr$ (Zindler & Hart 1986). **B** — $^{143}Nd/^{144}Nd_{(0)}$ vs. $^{147}Sm/^{144}Nd_{(0)}$ isotope correlation diagram with reference lines for calculated model ages of 355 Ma and 788 Ma, respectively. **C** — Diagram of initial $\varepsilon_{Nd(i)}$ and $\varepsilon_{Nd(t)}$ vs. $^{147}Sm/^{144}Nd$. **D** — Diagram of Nd isotope evolution against time (Ma). Diagram is showing depleted mantle model ages $T_{(DM2st)}$. Depleted Mantle curve according to Goldstein et al. (1984).

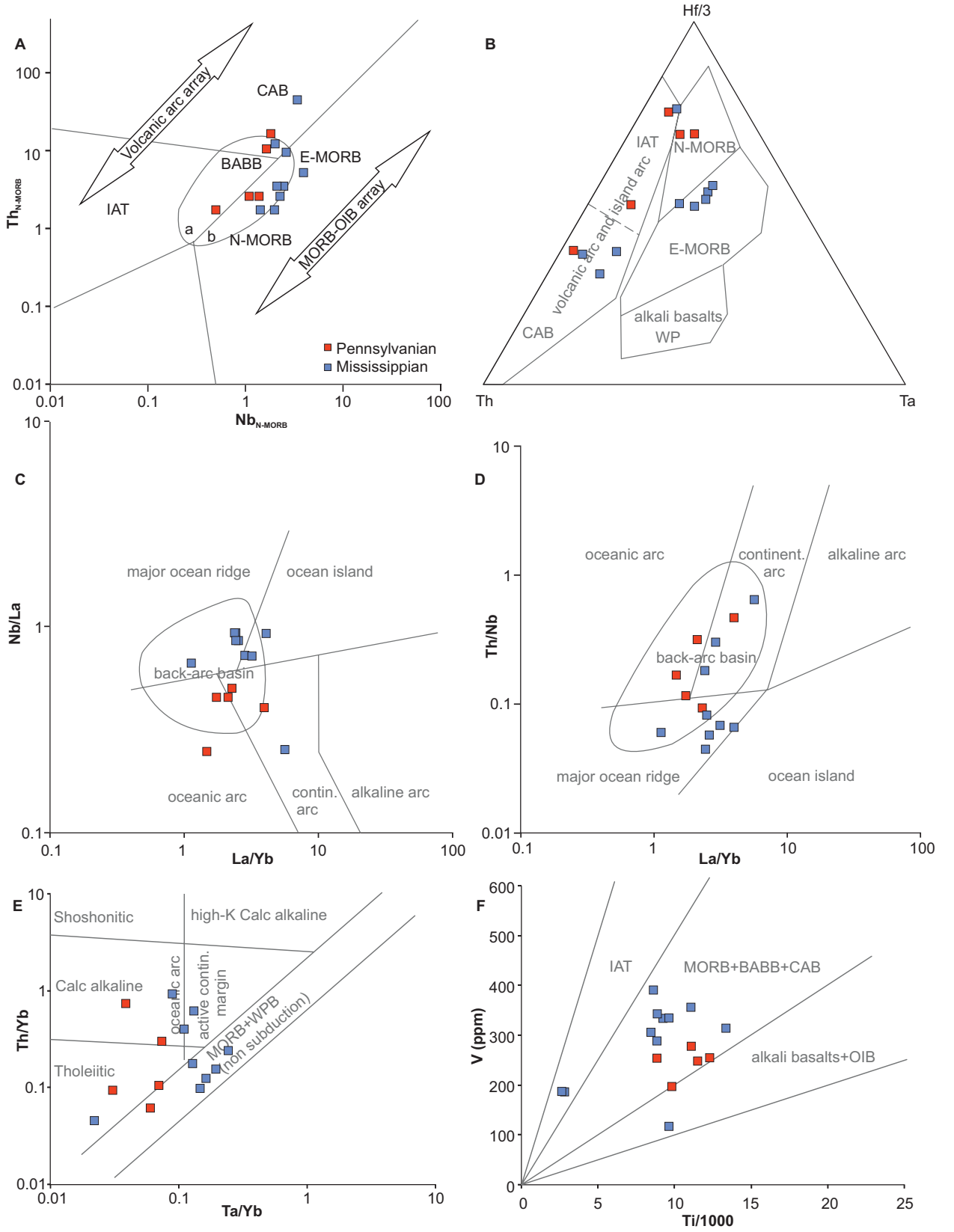


**Fig. 11.** Trace element discrimination diagrams for the petrogenetic and tectonic interpretation of the NGU Carboniferous metavolcanic rocks. **A** — Tectonic interpretation of ophiolitic basalts based on $Th_{N\text{-}MORB}$–$Nb_{N\text{-}MORB}$ systematics (after Saccani 2015); **B** — Hf–Th–Ta diagram (after Wood 1980); **C** — Nb/La–La/Yb discriminant diagram (after Hollocher et al. 2012); **D** — Th/Nb–La/Yb discriminant diagram (after Hollocher et al. 2012); **E** — Th/Yb–Ta/Yb discriminant diagram (after Pearce & Peate 1995); **F** — V vs. Ti/1000 metabasalt classification (after Shervais 1982)

and $(La/Yb)_N$ values (mean 1.60±0.68 and 1.64±0.75, respectively). A low degree of MREE and HREE fractionation is indicated by $(Tb/Yb)_N$ ratio values that range from 1.38 to 1.62 for Group I and from 0.92 to 1.35 for Group II. This is symptomatic of spinel-bearing peridotite-facies mantle, namely a mantle source devoid of residual garnet.

Contamination by continental crust leads to higher content of Th and elevated values of Th/Yb and Th/Nb (Wilson 1993; Pin & Paquette 1997; Pearce 2008, 2014 and references therein). Generally, all metabasalt samples display variation in depletion in Nb relative to La and Th (Th/Nb=0.17–0.45 in the Group I and 0.06–0.29 in Group II; La/Nb=2.03–4.08 and 1.07–1.41 respectively). The negative Nb, Ti anomalies and Th/Nb of <0.29 or even 0.45 could imply some crustal contribution to the magma. However, particularly elevated Th/Yb could be implied by incorporation of subduction-derived components. Consequently, the relatively high ratios of La/Yb (1.47–4.07 for Group I metabasalts versus 0.62–3.20 for Group II metabasalts), Nb/Zr (0.01–0.03 versus 0.01–0.07) and Nb/Y (0.03–0.15 versus 0.08–0.21) could indicate that the magma produced from a mantle wedge was metasomatized by slab melt source (e.g. Hawkesworth et al. 1997). The studied metabasites show a rather primitive chemical composition with not very pronounced signs of crustal assimilation. Hawkesworth et al. (1979, 1984) attributed this isotopic signature of the basalts to the character of mantle source and mantle metasomatism. Alternatively, Hofmann &White (1982) proposed that recycling of ancient oceanic crust into the OIB source could explain enrichment in trace elements and isotopes within the mantle array (subcontinental lithospheric mantle). New geophysical methods of mantle research have made it possible to explain the causes of uneven enrichment of depleted mantles by mantle convection models (e.g. Bunge et al. 1996; Forte & Mitrovica 2001).

On the selected discriminant diagrams (Fig. 11), it is possible to observe a relatively higher degree of enrichment of metabasites in Group I by elements indicating crustal assimilation compared to metabasalts in Group II. On the diagram Hf/3–Th–Ta (after Wood 1980) the studied metabasites fall into the N-MORB field, partially extending to the border with E-MORB, and shift significantly towards volcanic and island arc fields (Fig. 11). This transitional setting, that is intermediate between tholeiitic MORB and VAB-CAB patterns, having a smaller negative Nb anomaly is characteristic for back-arc tectonic setting (e.g. Pearce 1996, 2008; Pearce & Stern 2006; Dilek & Furnes 2009). A similar modification can be observed in the Nb/La vs. La/Yb and Th/Nb vs. La/Yb diagrams (after Hollocher et al. 2012 and references therein), which again indicate a back-arc setting (Fig. 11). However, the trend of differentiation also in the direction of the N-MORB/E-MORB towards the oceanic arc and even the continental arc in both observed groups of metabasites can be observed. The majority of the studied Mississippian metabasites are plotted in Th/Yb vs. Ta/Yb diagram (after Pearce 1983 and Pearce & Peate 2009) within the MORB-OIB array and conversely, Pennsylvanian metavolcanics are mostly shifted to the volcanic arc array (Fig. 11). This diagram illustrates the input of Th either from crustal contamination or its enrichment from the subduction zone. Similar differentiation is most visible on the $Th_N$–$Nb_N$ proxy (after Saccani 2016 based on Pearce 2008 proxies and references therein). The author defined two groups of back-arc type basic (BABB) volcanics: field **A** indicates BABB basalts characterized by input of subduction or crustal components and conversely, field **B** shows no input of crustal or subduction components. Based on $Th_N$–$Nd_N$ systematics the Pennsylvanian metabasites are predominantly plotted in the field **A** and the Mississippian in the field **B**.

The "depleted mantle" isotopic character of the studied metabasalts is indicated by relatively high $^{143}Nd/^{144}Nd_{(0)}$ ratio values, ranging between 0.51308 and 0.51302 for the Group I and between 0.51317 and 0.51287 for the Group II metabasalts. The problem is that the studied metabasalts have relatively high $^{87}Sr/^{86}Sr$ ratio values, in the range 0.7053–0.7081 for Group I and 0.7052–0.7076 for Group II. All studied samples have positive εNd(t) ranging from +8.25 to +8.54 for the Group I (t=320 Ma) and from +4.59 to +10.52 for the Group II (t=340 Ma) metabasalts (Tab. 4). In the light of these results, the isotopic variability of the given metabasalt suite was presumed. Their isotopic composition indicates (Fig. 10) the mixing array between prevalent mantle source (PREMA) and enriched mantle II (EM II), probably with influence of high U/Pb mantle component (HIMU), as was proposed for oceanic basalts suite by Zindler & Hart (1986). Horizontal array extending to high values of $^{87}Sr/^{86}Sr$ is documented by Worner et al. (1986) to assimilation of high-Sr crust by differentiated magma with very low Sr content due to plagioclase fractionation.

However, in both groups of metabasalts, an alternation has been observed of either weakly negative or slightly positive Nb anomalies, $(Nb/Th)_N$ from 0.26 to 1.31 in Group I and from 0.41 to 2.74 in Group II, at the same time at a highly positive value of εNd(t). On the other hand, all studied samples indicate low Th/Yb ratios (0.06–0.74 and 0.04–0.62, respectively). These low Th/Yb values, and at the same time relatively higher values of $(Nb/Th)_N$ ratios and positive εNd(t), indicate that their higher Th contents could be due to subducted-slab metasomatism (e.g. Pearce 1983; Pearce & Peate 1995) which is more likely than crustal contamination.

Volcanic rocks with mixed MORB and VAB composition are usually believed to be formed in supra-subduction zone such as fore-arc (e.g. Reagan et al. 2010; Morishita et al. 2011) or back-arc (e.g. Taylor & Martinez 2003; Sandeman et al. 2006) settings. Typical fore-arc basin volcanics are depleted in LREE in contrast to back-arc basin (Reagan et al. 2010; Johnson et al. 2014). It is true that Group II metabasalts are slightly depleted of LREE as well as Th, Ce and Rb compared to Group I metabasalts. In general, however, it is difficult to distinguish between the fore-arc and back-arc basalts if they are in a tectonic position near the suture in the arc-trench space of the convergent system (e.g. Pearce 2008; Saccani 2016). The back-arc **A** type volcanites are characterized by input of subduction or crustal components (Saccani 2016 and

references therein). In fact, based on $Hf_N/Sm_N$ vs. $Ta_N/La_N$ ratios (after La Flèche et al. 1998), both groups of metabasalts indicate subduction-related metasomatism; all these metabasalts were plotted in an area between melt or fluid-related subduction metasomatism and depleted mantle (Fig. 12). Generally, they exhibit low Th/Yb ratios (0.06–0.74 vs. 0.04–0.62, respectively) but highly variable Rb/Nb ratios, from 4.0 to 30.0 for Group I and from 0.15 to 1.73 for Group II metabasalts. It follows that Group I metabasalts are relatively more enriched in Th.

Group I metabasalts have $^{147}Sm/^{144}Nd_{(0)}$ ratios in the range of 0.1744 and 0.2003, which are lower or close to chondritic value of 0.1967. In contrast, Group II samples have highly variable $^{147}Sm/^{144}Nd_{(0)}$ ratios (0.1439–0.2402). In the conventional Sm–Nd isochron diagram (Fig. 10B), Group I metabasalts yield Sm–Nd isochron age of 355 Ma and Group II 788 Ma. Of course, it is older than the Pennsylvanian or Mississippian, as expected based on their occurrences (323.2±0.4 and 358.9±0.4 respectively; ICS 2019). A good grade of isotopic homogenization was found in both groups of volcanics, although each indicates a significantly different Sm–Nd isochron age. It is quite possible that the Sm–Nd system of the studied rocks had been slightly modified during regional greenschist metamorphism as is indicated by the increased LREE contents and at the same time low values of Nb/Th ratios, in the range of 0.38–1.31 for Group I and 0.41–2.14 for Group II metabasalts, which are more comparable to average crust (approximately 3; Taylor & McLennan 1985). The effect of crustal fluids is also indicated by higher Nd values (in ppm), which range from 13.5 to 16.4 in Group I and between 6.7 and 36.6 in Group II metabasalts.

Similarly, the apparent crustal residence ages, constrained by a two-stage Nd evolution model (recommended by Liew & Hofmann 1988), are clearly different between these two groups of metabasalts (Fig. 10D; Table 4). In Group I metabasalts the apparent crustal residence ages are relatively homogeneous ($t_{(DM2st)}$ = 0.39–0.36 Ga) and quite similar to the 355 Ma Sm–Nd isochron age calculated for t=320 Ma. Only one sample from the Group II is comparable to this, with $t_{(DM2st)}$ = 0.37 Ga ( sample *GZ-51*; Fig. 10; Table 4). These samples are considered cogenetic. The 0.39–0.36 Ga calculated $t_{(DM2st)}$ model ages for the Group I, as well as for one sample from the Group II metabasalts clearly indicate Hercynian juvenile magma derived from depleted mantle reservoir, relatively heterogeneous influenced by fluid-related subduction metasomatism (Fig. 12).

Significantly heterogeneous crustal residence ages prevailed in the rest of the Group II metabasalts, ranging from 0.54 to 0.84 Ga (Table 4) which overlap with the 788 Ma Sm–Nd isochrone age calculated for t=340 Ma. Thus, the $T_{DM}$ model ages are significantly older than the depositional age and apparently should not have geological meaning. Based on $(Hf/Sm)_{pm}$ vers. $(Ta/La)_{pm}$ ratios (after La Flèche et al. 1998), Group II metabasalts signalize MORB mantle source slightly enriched by subduction-related metasomatism (Fig. 12). Crustal contamination appears as a fairly limited process in these studied samples, whereas εNd values are positive. However, the existence of the old Cadomian crust is indicated by the spectra of detrital zircons in the metasediments of the underlying Rakovec Group. Two dominant assemblages of detrital zircon ages were documented in them, namely 0.545–0.640 Ga and 1.8–2.1 Ga (Vozárová et al. 2019b).

The range of the detected Nd model ages in the NGU Carboniferous metabasalts is very similar to those distinguished in the magmatic and metamorphic rocks of the Western Carpathians (Kohút et al. 1998, 1999; Poller et al. 2001, 2005; Gaab et al. 2005, 2006). The apparent crustal residence ages are comparable with others from the Hercynian belts of the Central Europe (e.g. Liew & Hofmann 1988; Janoušek et al. 1995).

The presence of two isotopically different groups of volcanics in the Mississippian sedimentary formation can be explained by its geological evolution. The preserved relics of the Mississippian sedimentary filling indicate deep-water turbidite sedimentation with metabasalts, serpentinites, and subordinate meta-andesites, amphibolites and carbonate olistoliths. It seems that most of the analysed samples are represented by the olistoliths of the older volcanics. Only one sample showed an isotopic composition identical to the Carboniferous ages of Group I volcanics, which documents, in addition to olistoliths, the coeval volcanism associated with the development of the Mississippian depositional realm.

This would rather suggest a tectonic position of fore-arc basin (Graham et al. 1975; Ingersoll et al. 1995, 2003; Ingersoll 2012). Equally, the spectrum of detrital zircons in the associated Mississippian sediments corresponds to the fore-arc tectonic position. The Mississippian detrital zircon population is characterized by the unimodal distribution, with a sharp age peak at 352 Ma (Vozárová et al. 2019a). These ages are close to the depositional age of the host sediments (~340 Ma). The Mississippian basin reflects derivation from a volcanic

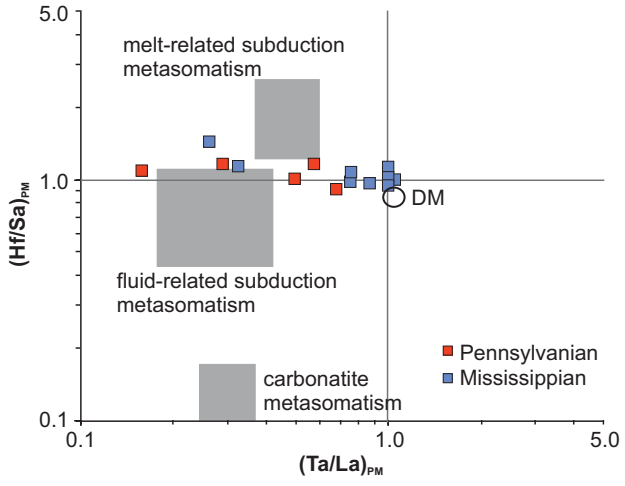


**Fig. 12.** $(Hf/Sm)_{PM}$ vs. $(Ta/La)_{PM}$ diagram for the NGU Carboniferous metabasalts, showing the field with indication of mantle source metasomatized by subduction-related processes (after LaFlèche et al. 1998).

arc that was nearly coeval with accumulation of sediments (Vozárová et al. 2019a).

The fragments of the Pennsylvanian basin fill are only insignificantly preserved in the Alpine structure of the NGU zone. Basal clastic sediments (the Rudňany Fm.), underlying the Zlatník volcanic horizon, contain fragments of Paleozoic ophiolites as well as fragments from the continental upper and lower crust (Vozárová 1973, 2001, 2005; Vozárová & Vozár 1988; Radvanec 1994). Similarly, detrital zircon assemblages, compared to Mississippian sediments, have shown a wider range: Devonian/Mississippian (364–351 Ma), Cambrian (510–534 Ma), Neoproterozoic (0.6–0.7 Ga), Paleoproterozoic (~2.0 Ga) and Neo-archean (2.6–3.0 Ga) (Vozárová et al. 2013; Vozárová et al. 2019a). If the Pennsylvanian sedimentary basin is interpreted as a back-arc, it would have to be situated close to the presumed suture. There is no doubt that the creation of the Pennsylvanian basin is associated with a collision and the subsequent creation of a basin system, both in the fore-arc and in the back-arc position to the assumed suture (Miall 1995; Ingersoll 2012 and references therein), which is difficult to define in today's NGU zone Alpine structure.

## Conclusions

The conclusions may be summarized as follows:

- The NGU Carboniferous metabasalts have both the MORB and VAB geochemical characteristics, and are likely to result from depleted mantle sources affected by fluid-related subduction metasomatism. They exhibit a broad spatial distribution, those with "arc" signatures ($Nb_N/Th_N$=0.2–1.0) for the Pennsylvanian (Group I) and "non-arc" signatures ($Nb_N/Th_N$=0.4–2.7) for the Mississippian (Group II) metabasalts. These geochemical attributes are interpreted as stemming from the transition from fore-arc to the initiation of extensional back-arc basin, associated with subduction zone.
- The Sm–Nd system specifies juvenile Nd isotope signatures with efficiencies of subducted-slab metasomatism; they are positive εNd(t) values, ranging from +8.25 to +8.54 for the Group I and from +2.98 to +6.56 for the Group II metabasalts. Sm–Nd isochron ages and $T_{DM}$ model ages for each of these suites are remarkable different. While the Sm–Nd isochron age of 0.355 Ga was determined for the Group I metabasalts, 0.788 Ga was found for the majority of the Group II metabasalts. $T_{DM2st}$ crustal residence ages are essentially identical with Sm–Nd isochron ages, 0.39–0.36 Ga and 0.54–0.82 Ga, respectively. These results indicate juvenile crustal addition during Hercynian and Cadomian orogenic events, thus the two groups of metabasalts are not cogenetic.
- Mixed metabasalts in Group II reflect the geological evolution of the Mississippian sedimentation basin, with deep-water turbidite sedimentation, in older metabasalts they appear as olistoliths. Coeval volcanism is documented by only one sample, with an isotopic composition indicating Hercynian events and are contemporary with Group I metabasalts.

**Acknowledgements:** The financial support of the Slovak Research and Development Agency (projects ID: APVV-0146-16) and of the Scientific Grant Agency of the Ministry of Education of the Slovak Republic and the Slovak Academy of Sciences (project VEGA 2/0006/19) is gratefully appreciated. The authors would like to thank M. Kohút and L. Krmíček for constructive reviews of the manuscript and for their helpful and critical comments and various hints on these topics.

## References

Abonyi A. 1971: Stratigraficko-tektonický vývoj karbónu gemeríd západne od štítnického zlomu. [Stratigraphic and tectonic evolution of the Gemeric Carboniferous west from the Štítnik Fault.] *Geologické Práce, Správy* 57, 339–348 (in Slovak).

Anczkiewicz A.A. & Anczkiewicz R. 2016: U–Pb zircon geochronology and anomalous Sr-Nd-Hf isotope systematics of late orogenic andesites: Pieniny Klippen Belt, Western Carpathians, South Poland. *Chemical Geology* 427, 1–16. https://doi.org/10.1016/j.chemgeo.2016.02.004

Andrusov D. 1959: Geológia československých Karpát, zväzok II. [Geology of the Czechoslovak Western Carpathians, 2nd part.] *VEDA Publishing House*, Bratislava, 1–376 (in Slovak).

Bajaník Š 1976: To petrogenesis of Devonian volcanic rocks of the Spišsko–gemerské rudohorie Mts. *Západné Karpaty: Séria Mineralógia, Petrografia, Geochémia* 2, 75–94.

Bajaník Š. & Planderová E. 1985: Stratigrafická pozícia spodnej časti ochtinského súvrstvia gemerika medzi Magnezitovcami a Magurou. [Stratigraphic position of the lower part of the Ochtiná Formation (between Magnezitovce and Magura).] *Geologické Práce, Správy* 82, 67–76 (in Slovak).

Bajaník Š., Vozárová A. & Reichwalder P. 1981: Litostratigrafická klasifikácia rakoveckej skupiny a mladšieho paleozoika v Spišsko-gemerskom rudohorí. [Lithostratigraphic classification of Rakovec Group and Late Paleozoic sediments in the Spišsko–gemerské rudohorie Mts.] *Geologické Práce, Správy* 75, 27–56 (in Slovak).

Bajaník Š., Hanzel V., Ivanička J., Mello J., Pristaš J., Reichwalder P., Snopko L, Vozár J. & Vozárová A. 1983: Explanation to geological map of the Slovenské rudohorie Mts. – eastern part. *D. Štúr Inst. Geol. Publ. House*, Bratislava, 3–223 (in Slovak with English summary).

Bajaník Š., Ivanička J., Mello J., Pristaš J., Reichwalder P., Snopko L., Vozár J. & Vozárová A. 1984: Geological map of the Slovenské rudohorie Mts. – eastern part, 1:50 000. *D. Štúr Inst. Geol.*, Bratislava.

Best M.G. & Christiansen E.H. 2000: Igneous Petrology. First Edition. *Wiley-Blackwell*, Malden, Massachusetts, 1–455.

Biely A., Bezák V., Elečko M., Gross P., Kaličiak M., Konečný V., Lexa J., Mello J., Nemčok J., Potfaj M., Rakús M., Vass D., Vozár J. & Vozárová A. 1996: Explanation to geological map of Slovakia, 1:500 000: *Dionýz Štúr Publisher*, Bratislava, 1–76.

Bouček B. & Přibyl A. 1960: Revise trilobitů slovenského svrchního karbonu. [Revision der Trilobiten aus dem slowakischen Oberkarbon.] *Geologické Práce, Správy* 20, 5–50 (in Czech with German summary).

Bucher K. & Grapes R. 2011: Petrogenesis of Metamorphic Rocks. 8th ed., *Springer-Verlag*, Berlin, Heidelberg, 1–428.

Bunge H.P., Richards M.A. & Baumgardner J.R. 1996: Effect of depth-dependent viscosity on the planform of mantle convection. *Nature* 379, 436–438.

Cathelineau M. 1988: Cation site occupancy in chlorites and illites as function of temperature. *Clay Minerals* 23, 471–485.

Dallmeyer R.D., Neubauer F., Handler R., Fritz H., Müller W., Pana D. & Putiš M. 1996: Tectonothermal evolution of the internal Alps and Carpathians: Evidence from $^{40}Ar/^{39}Ar$ mineral and whole rock data. *Eclogae Geologicae Helvetiae* 89, 203–227.

Dallmeyer R.D., Németh Z. & Putiš M. 2005: Regional tectonothermal events in Gemericum and adjacent units (Western Carpathians, Slovakia): Contribution by $^{40}Ar/^{39}Ar$ dating. *Slovak Geological Magazine* 11, 2-3, 155–163.

DePaolo D.J. 1981: Neodymium isotopes in the Colorado Front Range and crust–mantle evolution in the Proterozoic. *Nature* 291, 193–196.

DePaolo D.J. 1988: Neodymium Isotope Geochemistry: An Introduction. *Springer Verlag*, New York.

DePaolo D.J. & Wasserburg G.J. 1976: Nd isotopic variations and petrogenetic models. *Geophysical Research Letters* 3, 249–252.

Dilek Y. & Furnes H. 2009: Structure and geochemistry of Tethyan ophiolites and their petrogenesis in subduction rollback systems. *Lithos* 113, 1–20. https://doi.org/10.1016/j.lithos.2009.04.022

Dubacq B., Vidal O. & Andrade V. 2010: Dehydration of dioctahedral aluminous phyllosilicates: thermodynamic modelling and implications for thermo-barometric estimates. *Contributions to Mineralogy and Petrology* 159, 159–174. https://doi.org/10.1007/s00410-009-0421-6

Ebner F., Vozárová A., Kovács S., Kräutner H.-G., Krstić B., Szederkényi T., Jamićić D., Balen D., Belak M. & Trajanova M. 2008: Devonian–Carboniferous pre-flysch and flysch environments in the Circum Pannonian Region. *Geologica Carpathica* 59, 159–195.

Faryad S.W., Ivan P. & Jedlicka R. 2020: Pre-Alpine high-pressure metamorphism in the Gemer unit: mineral textures and their geodynamic implications for Variscan Orogeny in the Western Carpathians. *International Journal of Earth Sciences (Geol. Rundsch.)* 109, 1547–1564 (2020) https://doi.org./10.1007/s00531-020-01856-2

Faure G. 1986: Principles of Isotope Geology. 2nd ed., *Wiley,* New York, 1–589.

Fusán O. 1957: Paleozoic of Gemerides. *Geologické Práce, Zošit* 46, 17–36 (in Slovak).

Forte A.M. & Mitrovica J.X. 2001: Deep-mantle high viscosity flow and thermochemical structure inferred from seismic and geodynamic data. *Nature* 410, 1049–1055.

Gaab A., Poller U., Janák M., Kohút M. & Todt W. 2005: Zircon U–Pb geochronology and isotope characterization for the pre-Mesozoic basement of the Northern Veporic Unit (Central Western Carpathians, Slovakia). *Schweizerische Mineralogische und Petrographische Mitteilungen* 85, 69–88.

Gaab A., Janák M., Poller U. & Todt W. 2006: Alpine reworking of Ordovician photolith in the Western Carpathians: Geochronological and geochemical data on Muráň Gneiss Complex. *Lithos* 87, 261–274.

Goldstein S.J. & Jacobsen S.B. 1988: Nd and Sr isotopic systematic of rivers water suspended material: implications for crustal evolution. *Earth and Planetary Science Letters* 87, 249–265.

Goldstein S.J., O'Nions R.K. & Hamilton P.J. 1984: A Sm–Nd isotopic study of atmospheric dusts and particulates from major river systems. *Earth and Planetary Science Letters* 70, 221–236.

Graham S.A., Dickinson W.R. & Ingersoll R.V. 1975: Himalayan–Bengal model for flysch dispersal in Appalachian Quachita system. *Geological Society of America Bulletin* 86, 273–286.

Grecula M. 1998: Carboniferous of the Črmelicum terrane, Western Carpathians: relics of a fore-arc basin within Alpide Variscides. *Mineralia Slovaca* 30, 109–136.

Hawkesworth C.J., O'Nions R.K. & Arculus, R.J. 1979: Nd and Sr isotope geochemistry of island arc volcanics, Grenada, Lesser Antilles. *Earth and Planetary Science Letters* 45, 237–248.

Hawkesworth C.J., Rogers N.W., van Calsteren P.W.C. & Menzies M.A. 1984: Mantle enrichment processes. *Nature* 311, 331–333.

Hawkesworth C.J, Turner S., Peate D., McDermott F. & van Calsteren P. 1997: Elemental U and Th variations in island arc rocks: implications for U-series isotopes. *Chemical Geol*ogy 139, 207–221.

Hawthorne F.C., Oberti R., Harlow G.E., Maresch W.V., Martin R.F., Schumacher J.C. & Welch M.D. 2012: Nomenclature of the amphibole supergroup. *American Mineralogist* 97*,* 2031–2048. https://doi.org/10.2138/am.2012.4276

Hofmann A.W. & White W.M. 1982: Mantle plumes from ancient oceanic crust. *Earth and Planetary Science Letters* 57, 421–436.

Hollocher K., Robinson P., Walch E. & Roberts D. 2012: Geochemistry of amphibolite-facies of volcanics and gabbros of the Støren Nappe in extensions west and southwest of Trondheim, Western Gneiss Region, Norway: A key to correlations and palaeotectonic settings. *American Journal of Science* 312, 357–416. https://doi.org/10.2475/04.2012.01

Hovorka D., Ivan P., Jilemnická I. & Spišiak J. 1988: Petrology and geochemistry of metabasalts from Rakovec (Paleozoic of Gemeric Unit, Inner Western Carpathians). *Geologický Zborník Geologica Carpathica* 39, 395–425.

Hovorka D., Ivan P. & Méres Š. 1997: Leptyno-amphibolite complex of the Western Carpathians: Its definition, extent and genetical problems. In: Grecula P., Hovorka D. & Putiš M. (Eds.): Geological evolution of the Western Carpatians. *Mineralia Slovaca Monograph,* Košice, 269–280.

Hudáček J. 1963: Report on the geological map of area of the Mlynky – Biele Vody deposits. *Manuscript*, *Archives Geofond*, Bratislava (in Slovak).

Ingersoll R.V. 2012: Tectonic of sedimentary basins, with revised nomenclature. Chapter I. In: Busby C. & Pérez Azor A. (Eds.): Tectonics of Sedimentary Basins: Recent Advances. *Blackwell Publ. Ltd*., 3–43.

Ingersoll R.V., Graham S.A. & Dickinson W.R. 1995: Remnant ocean basins. In: Busby C.J. & Ingersoll R.V. (Eds.): Tectonics of sedimentary basins. *Oxford, Blackwell Science*, 363–391.

Ingersoll R.V., Dickinson W.R. & Graham S.A. 2003: Remnant-ocean submarine fans: largest sedimentary systems on Earth: In: Chan M.A. & Archer A.W. (Eds.): Extreme depositional environments: mega end members in geologic time. *Geological Society of America Special Papers* 370, 191–208.

Ivan P. 1994: Early Paleozoic of the Gemeric Unit (Inner Western Carpathians): Geodynamic setting as inferred from metabasalts geochemistry data. *Mitteilungen der Österreichischen Geologischen Gesellschaft* 86, 3–31.

Ivan P. 1997: Rakovec and Zlatník Formations: two different relics of the pre-Alpine back-arc basin crust in the Central Western Carpathians. In: Grecula P., Hovorka D. & Putiš M. (Eds.): Geological Evolution of the Western Carpathians: *Mineralia Slovaca, Monograph*, Bratislava, 281–288.

Ivan P. 2009: Early Palaeozoic basic volcanism of the Western Carpathians: geochemistry and geodynamic position. *Acta Geologica Universitatis Comenianae*, *Monogr. series*, Comenius University in Bratislava, 1–110 (in Slovak).

Ivan P. & Méres Š. 2012: The Zlatník Group – Variscan ophiolites on the northern border of the Gemeric Superunit (Western Carpathians). *Mineralia Slovaca* 44, 39–56.

Jacobsen S.B. & Wasserburg G.J. 1980: Sm-Nd isotopic evolution of chondrites. *Earth and Planetary Science Letters* 50, 139–155.

Janoušek V., Rogers G. & Bowes D.R. 1995: Sr–Nd isotopic constraints on the petrogenesis of the Central Bohemian pluton, Czech Republic. *Geologische Rundschau* 84, 520–534.

Johnson J.A., Hickey-Vargas R., Fryer P., Salters V. & Reagan M.K. 2014: Geochemical and isotopic study of a plutonic suite and related early volcanic sequences in the southern Mariana forearc. *Geochemistry, Geophysics, Geosystems* 15, 589–604.

Jowett E. 1991: Fitting iron and magnesium into the hydrothermal chlorite geothermometer. *Geol. Assoc. Canada/Miner. Assoc. Canada/Soc. Econ. Joint Annual Meeting. Toronto, May 27–29. Abstracts* 16, A62.

Kamenický L. & Marková M. 1957: Petrographic studies of the phyllite-diabase series of gemerides. *Geologické Práce, Zošit 45*, 111–189 (in Slovak).

Kohút M., Poller U., Todt W. & Janák M. 1998: Where are the roots of the Western Carpathians (Slovakia)? Evidence from isotope study. *POCEEL Praha, Acta Universitatis Carolinae, Geologica* 42, 277.

Kohút M., Kovach V.P., Kotov A.B., Salnikova E.B. & Savatenkov V.M. 1999: Sr and Nd isotope geochemistry of Hercynian granitic rocks from the Western Carpathians – implications for granite genesis and crustal evolution. *Geologica Carpath*ica 50, 477–487.

Kozur H. & Mock R. 1977: Erster Nachweis von Conodonten im Paleozoikum (Karbon) der Westkarpaten. *Časopis pro mineralogii a geol*ogii 22, 299–305.

Kozur H., Mock R. & Mostler H. 1976: Stratigraphische Neueinstufung der Karbonatgesteine der unteren Schichtenfolgen von Ochtiná (Slovakei) in das oberste Vise-Serpukhovian (Namur A). *Geologisch-Paläontologische Mitteilungen* 6, 1–29.

Krist E. 1954: Bindt-Rudňany conglomerates, Carboniferous of the northern part of the Slovenské Rudohorie Mts. *Geologické Práce, Zošit* 36, 77–107 (in Slovak).

LaFlèche M.R., Camiré G. & Jenner G.A. 1998: Geochemistry of post-Acadian, Carboniferous continental intraplate basalts from Maritimes Basin, Magdalen Islands, Québec, Canada. *Chemical Geology* 148, 115–136.

Leake B.E., Woolley A.R., Arps C.E.S., Birch W.D., Gilbert M.C., Grice J.D., Hawthorne F.C., Kato A., Kisch H.J., Krivovichev V.G., Linthout K., Laird J., Mandarino J.A., Maresch W.V., Nickel E.H., Schumacher J.C., Smith D.C., Stephenson N.C.N., Ungaretti L., Whittaker E.J.W. & Youzhi G. 1997: Nomenclature of Amphiboles. *Canadian Mineralogist* 35, 219–246.

Liew T.C. & Hofmann A.W. 1988: Precambrian crustal components, plutonic associations, plate environment of the Hercynian Fold Belt of Central Europe: Indications from a Nd and Sr isotopic study. *Contributions to Mineralogy and Petrology* 98, 129–138.

Locock A.J. 2014: An Excel spreadsheet to classify chemical analyses of amphiboles following the IMA 2012 recommendation. *Computers & Geosciences* 62, 1–11.

Maheľ M. 1983: The Northern Gemeric synclinal and the Besník Nappe – an example of interconnections of superficial and deep structural elements. *Mineralia Slovaca* 15, 1–22 (in Slovak).

Mamet B. & Mišík M. 2003: Marine Carboniferous algae from metacarbonates of Ochtiná Formation (Gemeric Unit, Western Carpathians). *Geologica Carpathica* 54, 3–8.

Máška M. 1959: Research report on the Paleozoic of the Spiš-Gemer Ore Mountains (III. Carbon in total). *Zprávy o geologických výzkumech (Ústř. Úst. Geol.) 1957*, 136–146 (in Czech).

Miall A.D. 1995: Collision-related foreland basins. In: Busby C.J. & Ingersoll R.V. (Eds.): Tectonics of sedimentary basins. *Blackwell Science*, Oxford, 393–424.

Morishita T., Dilek Y., Shallo M., Tamura A. & Arai S. 2011: Insight into the uppermost mantle section of a maturing arc: The Eastern Mirdita ophiolite, Albania. *Lithos* 124, 215–226.

McDonough W.F. & Sun S-S 1995: The composition of the Earth. *Chemical Geology* 120, 223–253.

Němejc F. 1947: Contribution to knowledge of floral remnants and stratigraphical division of Permo-Carboniferous of Slovakia. *Rozpravy II. České Akademie Věd* 56, 1–34 (in Czech).

Németh Z. 2002: Variscan suture zone in Gemericum: Contribution to reconstruction of geodynamic evolution and metallogenic events of Inner Western Carpathians. *Slovak Geological Magazine* 8, 247–257.

Németh Z., Procházka W., Radvanec M., Kováčik M., Madarás J., Koděra P. & Hraško Ľ. 2004: Magnesite and talc origin in the sequence of geodynamic events in Veporicum, Inner Western Carpathians. *Acta Petrologica Sinica* 20, 837–854.

Neubauer F. & Vozárová A. 1990: The Noetsch-Veitsch-Northgemeric Zone of Alps and Carpathians: Correlation, paleogeography and significance for Variscan orogeny. In: Minaříková D. & Lobitzer H. (Eds.): Thirty years of geological cooperation between Austria and Czechoslovakia. *Federal Geological Survey*, Vienna, 167–171.

Ogurčák Š. 1954: Report on geological mapping in the vicinity of Mlynky village. *Manuscript, Archives Geofond*, Bratislava (in Slovak).

Parra T., Vidal O. & Agard P.A 2002: Thermodynamic model for Fe–Mg dioctahedral K white micas using data from phase-equilibrium experiments and natural pelitic assemblages. *Contributions to Mineralogy and Petrology* 143, 706–732.

Patchett P.J. & Arndt N.T. 1986: Nd isotopes and tectonics of 1.9–1.7 Ga crustal genesis. *Earth and Planetary Science Letters* 78, 329–338.

Pearce J.A. 1982: Trace element characteristics of lavas from destructive plate boundaries. In: Thorpe R.S. (Ed.): Orogenic Andesites. *Wiley*, Chichester, 528–548.

Pearce J.A. 1983: Role of the subcontinental lithosphere in magma series at active continental margins. In: Hawkesworth C.J. & Norry M.J. (Eds.): Continental Basalts and Mantle Xenoliths. *Shiva*, Nantwitch, 230–249.

Pearce J.A. 1996: A User's Guide to basalt Discrimination Diagrams. In: Wymann D.A. (Ed.): Trace Element geochemistry of Volcanic rocks: Applications for Massive Sulphide Exploration. *Short Course Note* 12, 79–113.

Pearce J.A. 2008: Geochemical fingerprinting of oceanic basalts with applications to ophiolite classification and to search for Archean oceanic crust. *Lithos* 100, 14–43. https://doi.org/10.1016/j.lithos.2007.06.016

Pearce J.A. 2014: Immobile element fingerprinting of ophiolites. *Elements* 10, 101–108. https://doi.org/10.2113/gselements.10.2.101

Pearce J.A. & Peate D.W. 1995: Tectonic implications for the composition of volcanic arc magmas. *Annual Review of Earth and Planetary Sciences* 23, 251–285.

Pearce J.A. & Stern R.J. 2006: Origin of back-arc basin magmas: trace element and isotope perspectives. *AGU Geophysical Monograph Series* 166, 63–86.

Pecho J. & Popreňák J. 1962: Geological-tectonic structure in the vicinity of Rudňany village and its relation to mineralization. *Geologické Práce, Zošit* 61, 223–234 (in Slovak).

Pin C. & Paquette J.L. 1997: A mantle-derived bimodal suite in the Hercynian Belt: Nd isotope and trace element evidence for a subduction-related rift origin of the Late Devonian BreÂvenne metavolcanics, Massif Central (France). *Contributions to Mineralogy and Petrology* 129, 222–238.

Planderová E. & Vozárová A. 1982: Biostratigraphical correlation of the Late Paleozoic formations in the West Carpathians. In: Sassi F.P. (Ed*.): Newsletter No. 4, IGCP Project No. 5*, Padova, 67–71.

Plašienka D. 2018: Continuity and episodicity in the early Alpine tectonic evolution of the Western Carpathians: How large-scale processes are expressed by the orogenic architecture and rock record data. *Tectonics* 37, 2029–2079. https://doi.org/10.1029/2017TC004779

Poller U., Todt W., Kohút M. & Janák M. 2001: Nd, Sm, Pb isotope study of the Western Carpathians: implication for Palaeozoic evolution. *Schweizerische Mineralogische und Petrographische Mitteilungen* 81, 159–174.

Poller U., Kohút M., Gaab A. & Todt W. 2005: Pb, Sr, Nd isotope study of two co-existing magmas in the Nízke Tatry Mts., Western Carpathians (Slovakia). *Mineralogy and Petrology* 84, 215–231.

Polák M. & Jacko S. et al. 1996: Geological map of the Branisko and Čierna Hora Mts. *Geol. Surv. Slovak Rep.,* Bratislava.

Putiš M., Ivan P., Kohút M., Spišiak J., Siman P., Radvanec M., Uher P., Sergeev S., Larionov A., Méreš Š., Demko R. & Ondrejka M. 2009a: Meta-igneous rocks of the West-Carpathian basement, Slovakia: indicators of Early Paleozoic extension and shortening events. *Bulletin de la Societé géologique de France* 180, 6, 461–471.

Putiš M., Frank W., Plašienka D., Siman P., Sulák M. & Biroň A. 2009b: Progradation of the Alpidic Central Western Carpathians orogenic wedge related to two subductions: constrained by $^{40}Ar/^{39}Ar$ ages of white micas. *Geodinamica Acta* 22, 31–56.

Radvanec M. 1994: Petrology of the Gemeric gneiss-amphibolite complex, northern part of the Rudňany deposits. Part I: P-T-x conditions and zonality of metamorphism. *Mineralia Slovaca* 26, 223–238.

Radvanec M., Németh Z., Kráľ J. & Pramuka S. 2017: Variscan dismembered metaophiolite suite fragments of Paleo-Tethys in Gemeric unit, Western Carpathians. *Mineralia Slovaca* 49, 1–48.

Rakusz Gy. 1932: Die oberkarbonischen Fossilien von Dobšiná und Nagyvisnyó. *Geologica Hungarica, Series Palaeontologica* 8, 1–219.

Reagan M.K., Ishizuka O., Stern R.J., Kelley K.A., Ohara Y., Blichert-Toft J., Bloomer S.H., Cash J., Fryer P. & Hanan B.B. 2010: Fore-arc basalts and subduction initiation in the Izu–Bonin–Mariana system. *Geochemistry, Geophysics, Geosystems* 11, 17. https://doi.org/10.1029/2009GC002871

Rozložník L. 1963: Basic volcanites in the Dobšiná Carboniferous facies. *Geologické Práce, Správy* 27, 35–48 (in Slovak).

Russell W.A., Papanastassiou D.A. & Tombrello T.A. 1978: Ca isotope fractionation on the Earth and other solar system materials. *Geochimica et Cosmochimica Acta* 42, 1075–1090.

Saccani E. 2015: A new method of discriminating different of post-Archean ophiolitic basalts and their tectonic significance using Th–Nb and Ce–Dy–Yb systematics. *Geoscience Frontiers* 6, 481–501.

Sandeman H., Hanmer S., Tella S., Armitage A., DavisW. & Ryan J. 2006: Petrogenesis of Neoarchaean volcanic rocks of the MacQuoid supracrustal belt: a back-arc setting for the northwestern Hearne subdomain, western Churchill Province, Canada. *Precambrian Research* 144, 140–165.

Shervais J.W. 1982: Ti–V plots and the petrogenesis of modern and ophiolitic lavas. *Earth and Planetary Science Letters* 59, 101–118.

Snopková P. 1978a: Report on the evaluation of palynological samples for Project no. 122. *Manuscript*, *Archives of D. Štúr Institute of Geology*, Bratislava (in Slovak)

Snopková P. 1978b: Annual report on the research of the Črmeľ Serie. *Manuscript*, *Archives of D. Štúr Institute of Geology*, Bratislava (in Slovak)

Spišiak J., Hovorka D. & Ivan P. 1985: Klátov Group the representative of the Paleozoic amphibolite facies metamorphites of the Inner Western Carpathians. *Geologické Práce, Správy* 82, 205–220 (Slovak with English summary).

Sun S-S. & McDonough W.F. 1989: Chemical and isotope systematic of oceanic basalts implications for mantle composition and processes. In: Sounders A.D. & Norry M.J. (Eds.): Magmatism in ocean basins. *Geological Society, London, Special Publications* 42, 313–345.

Taylor B. & Martinez F. 2003: Back-arc basin basalt systematics. *Earth and Planetary Science Letters* 210, 481–497.

Taylor S.R. & McLennan S.M. 1985: The Continental Crust: its Composition and Evolution. *Blackwell Science*, Oxford.

Tischendorf G., Förster H.-J., Gottesmann B. & Rieder M. 2007: True and brittle micas: composition and solid-solution series. *Mineralogical Magazine* 71*,* 285–320.

Vidal O., De Andrade V., Lewin E., Munoz M., Parra T. & Pascarelli S. 2006: P–T-deformation–Fe3+/Fe2+ mapping at the thin section scale and comparison with XANES mapping: application to a garnet-bearing metapelite from the Sambagawa metamorphic belt (Japan). *Journal of Metamorphic Geology* 24, 7, 669–683.

Vozárová A. 1973: Pebble analysis of the late Paleozoic conglomerates in Spišsko–Gemerské rudohorie Mts. *Geologický Zborník Západné Karpaty* 18, 7–98 (in Slovak).

Vozárová A. 1996: Tectono-sedimentary evolution of Late Paleozoic basins based on interpretation of lithostratigraphic data (Western Carpathians; Slovakia). *Slovak Geological Magazine* 3–4, 251–271.

Vozárová A. 2001: Plagiogranite pebbles in Westphalian conglomerates of the Northern Gemericum Unit: their characteristic and geotectonic significance (Western Carpathians). *Krystalinikum* 27, 79–88.

Vozárová A. & Vozár J. 1988: Late Paleozoic in West Carpathians. *D. Štúr Institute of Geology*, Bratislava, 1–314.

Vozárová A., Frank W., Kráľ J. & Vozár J. 2005: $^{40}Ar/^{39}Ar$ dating of detrital mica from the Upper Paleozoic sandstones in the Western Carpathians (Slovakia). *Geologica Carpathica* 56, 463–472.

Vozárová A., Laurinc D., Šarinová K., Larionov A., Presnyakov S., Rodionov N. & Paderin I. 2013: Pb ages of detrital zircons in relation to geodynamic evolution: Paleozoic of the Northern Gemericum (Western Carpathians, Slovakia). *Journal of Sedimentary Research* 83, 915–927. https://doi.org/10.2110/jsr.2013.66

Vozárová A., Konečný P., Šarinová K. & Vozár J. 2014: Ordovician and Cretaceous tectonothermal history of the Southern Gemericum Unit from microprobe monazite geochronology (Western Carpathians, Slovakia). *International Journal of Earth Sciences* (*Geol. Rundsch.*) 103, 1005–1022. https://doi.org/10.1007/s00531-014-1009-6

Vozárová A., Šarinová K., Laurinc D., Lepekhina E., Vozár J., Rodionov N. & Lvov P. 2019a: Exhumation history of the Variscan suture: Constrains on the detrital zircon geochronology from Carboniferous–Permian sandstones (Northern Gemericum; Western Carpathians). *Geologica Carpath*ica 70, 512–530. https://doi.org/10.2478//geoca-2019-0030

Vozárová A., Rodionov N. & Šarinová K. 2019b: Recycling of Paleoproterozoic and Neoproterozoic crust recorded in Lower Paleozoic metasandstones of the Northern Gemericum (Western Carpathians, Slovakia): Evidence from detrital zircons. *Geologica Carpathica* 70, 298–310. https://doi.org/10.2478/geoca-2019-0017

Wasserburg G.J., Jacobsen S.B., DePaolo D.J., McCulloch M.T. & Wen T. 1981: Precise determination of Sm/Nd ratios, Sm and Nd isotopic abundances in standard solutions. *Geochimica et Cosmochimica Acta* 45, 2311–2323.

Wilson B.M. 1989: Igneous Petrogenesis: A Global Tectonic Approach. *Unwin Hyman*, London, 1–466.

Wilson B.M. 1993: Igneous petrogenesis: a global tectonic approach. *Chapman and Hall*, London, 1–466.

Winchester J.A. & Floyd P.A. 1977: Geochemical discrimination of different magma series and their differentiation products using immobile elements. *Chemical Geology* 20, 325–343.

Wood D.A. 1980: The application of a Th-Hf-Ta diagram to problems of tectonomagmatic classification and to establishing the nature of crustal contamination of basaltic lavas of the British Tertiary Volcanic Province. *Earth and Planetary Science Letters* 50, 11–30.

Worner G., Zindler A., Staudigel H. & Schmincke H.-U. 1986: Sr, Nd, and Pb isotope geochemistry of Tertiary and Quaternary alkaline volcanics from West Germany. *Earth and Planetary Science Letters* 79, 107–119.

Yavuz F., Kumral M., Karakaya N., Karakaya M. & Yildirim D.A. 2015: Windows program for chlorite calculation and classification. *Computers & Geosciences* 81, 101–113.

Zágoršek K. & Macko A. 1994: Carboniferous Bryozoa from the Jedlovec quarry in Ochtiná Formation (Gemericum, Western Carpathians): *Mineralia Slovaca* 26, 5, 335–346.

Zane A. & Weiss Z. 1998: A procedure for classifying rock-forming chlorites based on microprobe data. *Rendiconti Lincei. Scienze Fisiche e Naturali* 9, 51–56. https://doi.org/10.1007/BF02904455

Zindler A. & Hart S.R. 1986: Chemical geodynamics. *Annual Review of Earth and Planetary Sciences* 14, 493–571.

**Supplementary Tables S1–S4** are available online at http://geologicacarpathica.com/data/files/supplements/GC-72-2-Vozarova_Suppl_Tables_S1-S4.xlsx.